Physics Theses & Dissertations   Physics

Summer 2016

Discipline-Based Planetary Education Research and Computational Fluid Dynamics Analysis of Mars

Filis Coba
Old Dominion University

Follow this and additional works at: https://digitalcommons.odu.edu/physics_etds

Part of the Astrophysics and Astronomy Commons, Geophysics and Seismology Commons, Science and Mathematics Education Commons, and the Tectonics and Structure Commons

DISCIPLINE-BASED PLANETARY EDUCATION RESEARCH AND COMPUTATIONAL FLUID DYNAMICS ANALYSIS OF MARS

by

Filis Coba
B.S. December 2010, Central Connecticut State University

A Thesis Submitted to the Faculty of
Old Dominion University in Partial Fulfillment of the
Requirements for the Degree of

MASTER OF SCIENCE

PHYSICS

OLD DOMINION UNIVERSITY
August 2016

Approved by:

Declan De Paor (Director)

Jennifer Georgen (Co-Director)

Gail Dodge (Member)

ABSTRACT

DISCIPLINE-BASED PLANETARY EDUCATION RESEARCH AND COMPUTATIONAL FLUID DYNAMICS ANALYSIS OF MARS

Filis Coba
Old Dominion University, 2016
Director: Dr. Declan De Paor
Co-Director: Dr. Jennifer Georgen

This thesis originates from the testing and implementation of an IRB-approved interactive animation designed to help students understand what causes The Reasons For The Seasons (RFTS) on Earth. Results from the testing indicated a small improvement in student understanding after exposure to the animation. Next, using the 3-D mapping tool Google Earth, students explored seasons and other planetary features on Mercury, Venus, the Moon and Mars through IRB-approved interactive tours which were developed and tested for astronomy education. Results from the tests indicated that there were statistically significant learning gains (p-value < 0.05) after students interacted with the tours compared to those who did not. The development of the tours inspired a geophysics study of the possibility of former plate motion (or plate tectonics) on Mars. A 2-D finite element convection model for the mantle of Mars was designed and solved using COMSOL Multiphysics 5.1, to investigate whether or not thermal gradients in a Mars-sized planet could cause vigorous upper mantle convection, consistent with plate tectonic processes. Results from this project indicated that stable convection could occur in the interior of a Mars-like planet assuming the presence of sufficiently high thermal gradients at about 0.8 times the mantle temperature of Earth. The convective patterns resembled hot upwelling and cool downwelling which may be similar to subduction-like features. Furthermore, increasing the temperature of the hot boundaries resulted in faster, more rigorous convective motions and a hotter average temperature.

ACKNOWLEDGEMENTS

PREFACE

This thesis contains a sequence of planetary science studies beginning with discipline-based education research (DBER) and culminating in a computational fluid dynamics (CFD) research project involving Mars. This progression aligns with the geospatial visualization program whereby education research leads to the investigation of geophysical research questions, which can be further explored.

Students commonly think that Earth's seasons are caused by the distance from the Sun. To mitigate this misconception, an IRB-approved interactive visualization was tested to see whether interactivity helped students understand what causes The Reasons For The Seasons (RFTS) on Earth (De Paor et al., 2016b), shown in Fig. 1. Students see that the ecliptic is tilted with respect to the equator, which changes both the length of the day and the position of the Sun in the sky. This study is not included in the main body of the thesis since the majority of the author's contribution to this project was through testing and scoring. In a classroom test of 27 students, 15 students improved their scores after interacting with the animation, seven students remained unchanged, and five students scored worse (Fig. 2). This hints that interactive activities may provide greater learning gains over traditional media.

Similarly, interactive planetary tours of Mercury, Venus, Earth's Moon, and Mars were developed using Google Earth. Learning objectives, lesson plans, and detailed user guides pertaining to each tour were also designed. Google Earth is a powerful instructional resource for geoscience education, and virtual planetary research and exploration. One of the most useful features is the users' ability to image-overlay the latest 2-D topological, crustal, and gravitational maps (from NASA, ESA, and other sources) directly onto a 3-D view of the planet's surface, thereby transforming it. Viewing data this way captures the truest essence of reality, and thus is quite useful in planetary science. Being able to pan, zoom, and change the camera angle helped identify hidden patterns, providing more information on the surface, and indirectly on the interior of a planet. Ultimately, it was viewing Mars in such a visually artistic way that coalesced a Martian geophysical research topic.

Downloadable files associated with this part of the thesis include lessons about the terrestrial planets, and links made available in Appendix 2.5. Inspired by the famous 17th Century European "Grand Tour" trips, our planetary tours were designed to help students explore atmospheres, interiors, magnetospheres, and landscapes.

Development of the tours benefitted from a study of 364 students in Physics 103, an introductory astronomy class at Old Dominion University, where the learning outcomes were
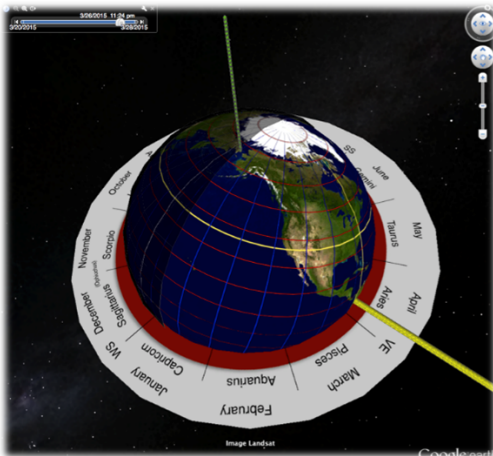
3D Model of Ecliptic Plane

FIG. 1: 3D model of the ecliptic place in Google Earth. Grid = right ascension / declination. Yellow line = sunbeam, green = ecliptic pole. Nighttime hemisphere shaded.

Post-Test Versus Pre-Test in RFTS
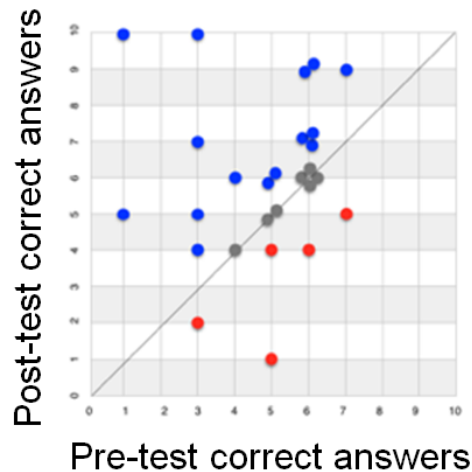
FIG. 2: Individual students' post-test versus pre-test scores in RTFS. Blue dots show improved results, grey dots show unchanged results, and red dots show worsened results.

compared for students using Google Earth versus static PDF files, with IRB approval number 644253-1. In pre- and immediate post-tests, there were small but statistically significant (p-value < 0.05) learning gains from use of Google Earth, although these did not persist in a longterm follow-up. Results suggested (De Paor et al., 2016a), that there were insufficient differences between viewing text and images in Google Earth placemark balloons versus identical text and images in a PDF document. Consequently, the tours were revised, and included many more 3-D COLLADA models, draped maps, and movies to the KML version. The first chapter of this thesis is a summary of that paper. Results of this study were also presented by F. Coba at the annual meeting of the Northeast Section of the Geological Society of America in 2015.

Upon creating the Martian tour stop for gravity, the gravitational anomaly map was examined. How much influence does gravity have on the construction and reconstruction of a planets surface? The next thesis chapter investigates gravitationally-driven fluid flow in the upper mantle of a Mars-like planet. Earth is the only planet on which there is evidence for current plate tectonics. The history of Martian tectonics is less well understood. It is well known that mantle plume tectonics dominated the Hesperian and Amazonian Periods (3.7 b.y. to present) on Mars, but it is also hypothesized that plate tectonics may have occurred

in the Pre-Noachian (4.56 – 4.1 b.y.) shown in Fig. 3. The evidence in favor of plate tectonics on Mars is based on the existence of magnetic stripes similar to those in Earths oceans that are partially obliterated by the Noachian Late Heavy Bombardment. However, there are no jigsaw shaped conjugate continental margins like on Earth. Non-plate tectonic models have been proposed for the development of the Tharsis region and the crustal dichotomy (Reese & Solomatov, 2006). Zhong (2009) has argued that Mars cannot have large-scale motion of the lithosphere according to the standard theory of stagnant-lid convection.
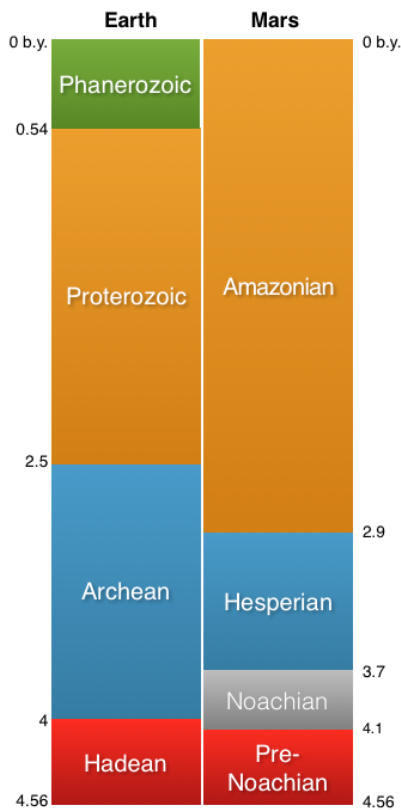
Geologic Eras on Earth and Mars

FIG. 3: Comparison of geologic eras on Earth (left) and on Mars (right). Fig. from (De Paor et al., 2016a)

TABLE OF CONTENTS

LIST OF TABLES

LIST OF FIGURES

CHAPTER 1

A GOOGLE EARTH GRAND TOUR OF THE TERRESTRIAL PLANETS

1.1 ABSTRACT

The popularity of animations and interactive visualizations in undergraduate science education might lead one to assume that these teaching aids enhance student learning. We tested this assumption for the case of the Google Earth virtual globe with treatment and comparison student groups in a general education class of over 370 students at a large public university. Earth and Planetary Science course content was developed in two formats: using Keyhole Markup Language (KML) to create interactive tours in Google Earth (the treatment group) and Portable Document Format (PDF) for on-screen reading (the comparison group). The PDF documents contained the static equivalents of the images found in the placemark balloons or "tour stops" in the Google Earth version. Student learning was tested with pre-and post-questionnaires and long-term retention was assessed with a follow-up post-questionnaire 11 weeks later. Some significant differences were noted between the two groups based on the immediate post-questionnaire with the KML students out-performing the PDF students, but not on the delayed measure (In fact, the PDF group fared slightly better but that was not statistically significant). Additionally, we observed student behavior during the activities and interviewed a small subset of students (N=3). Although 17 students signed up for the interview, only three students showed up. Those students who did participate in general were more engaged when using Google Earth. Students we interviewed had mixed feelings regarding the benefits of KML over PDF.

1.2 INTRODUCTION

Generations of students have experienced the traditional chalkboard style of teaching along with reading assignments, problem sets, and laboratory exercises. "Chalk-and-talk" has its defenders (e.g., Ressler, 2004; Sewasew et al., 2015), however digital technology such as PowerPoint plays an increasing role in classrooms today and its effectiveness is a topic

of ongoing study. In today's society, teachers are competing against cellphones for the attention of their students. Students who are ill-prepared for college, or poorly for learning, may be difficult to engage. Mandatory general education science courses present a particular challenge.

This project was motivated by the following questions: 1) How much do students benefit from interactive computer graphics when learning earth and planetary science? 2) Which delivery medium will yield long term learning retention if any? This study investigated specifically whether students would benefit from hands-on, interactive learning using Google Earth virtual globe software in an on-site, collaborative learning classroom. Would there be increased enthusiasm and better learning outcomes in this student group composed of non-science majors by introducing Google Earth at those stations? The goal was to compare the learning outcomes of static PDF text and images (there was no 3D PDF content) to interactive KML content delivered in Google Earth with the same text and images in geo-referenced placemark balloons.

1.3 SETTING OF STUDY

This project studied a class of over 370 students from Old Dominion University. The undergraduate population of about 25,000 students is 54% female, 22% African American, 25% military affiliated, approximately a third residential and two-thirds commuters or distance learners. All but a handful of the class were non-science majors pursuing general education requirements.

The class was one of two introductory astronomy course offered on-site by the Physics Department: "Stars and Galaxies" and "Solar System." The semester in question concentrated on the solar system, especially terrestrial planets, Earth, and Earth's Moon (henceforth grouped with the terrestrial planets).

Students in the laboratory sections for this course sometimes watched planetarium full-dome digital presentations delivered by their TA and answered follow-up questions. They also participated in other hands-on laboratory activities.

The class was divided into 12 laboratory sections with approximately 32 students per section. There was also one section with 12 students restricted to the university's Honors College. Students worked in groups of three per computer (Fig. 4). Total student participation, accounting for absentees and those who declined to participate under IRB-compliant consent was 364.

Laboratory set-up

FIG. 4: Laboratory set-up. Three students were assigned to each of 12 iMac computers, each with one keyboard and two mice. Image credit given to Justin Mason, Director of Pretlow Planetarium at Old Dominion University.

1.4 EXPERIMENTAL DESIGN

Each laboratory section was divided into lab-bench workstations using PDF documents and an equal number using Google Earth KML files to study the same terrestrial body. KML files were loaded into Google Earth, and PDF documents were placed on the computer desktop prior to the start of class in order to minimize set-up instructions for students, none of which was revealed to the students prior to the study. The computer monitors were turned off, and if paper instructions were on the computer table, they were turned over to a blank side.

As soon as students walked into lab, their sign-in sheet asked that they create a unique four-digit pin number next to their name, which they can easily remember. Initially students sat in movie-theatre style planetarium seats and it was there they were asked to sign an IRB form and that they would take a (closed book, closed phone) pre-test measuring their knowledge on the terrestrial planets in our solar system and our Moon. They were given roughly 25 minutes to complete the pre-test. If they finished early, they were asked to turn their paper over and quietly wait for the other students to finish. Once time was up, the pre-tests were collected.

Only when the study began were the students asked to sit at the computer tables and

FIG. 5: Tour style schedule for each lab section. The schedule was designed such that four classes received all Google Earth tours of each terrestrial body, four different classes received all PDF tours of each planet and the Moon, and the four remaining lab classes had half PDF and half Google Earth tours.

work in groups of three. Students chose which computer station to sit at and which members of the class to work with, not knowing whether it was a treatment or comparison computer. In case there was any unfamiliarity with Google Earth, the KML group received a set of basic instructions on how to start up and navigate. They were told to share the control of the keyboard, and two mice in total were attached to each keyboard (Fig. 4).

The students in each lab were given about 35-40 minutes to go through the tour. Once they were done, they shut off their screens and took a post-test. All the tests in the KML group section were placed in a sealed envelope labeled with the TA's name, lab section, date and time but not labeled KML. It was important for the scorer to be unaware if the test was from a KML or PDF group while scoring each envelope to limit any initial bias. As such, in addition to matching the pin numbers, a master schedule of which TA and lab section received which planet and tour style shown in Fig. 5, was created prior to the study and was used only when administering the tours and after grading the tests.

The schedule was designed such that four classes received all Google Earth tours of each planet and the Moon, four different classes received all PDF tours of each planet and the Moon, and the four remaining lab classes had half PDF and half Google Earth tours of each

Google Earth Placemark

FIG. 6: Example of Google Earth placemark balloon with text and images. Terrain imagery for Venus was created by De Paor et al. 2012 based on NASA's SARS mission.

planet and the Moon. The tests were scored one envelope at a time using specific rubrics.

The KML tours consisted of a series of Google Earth placemarks located on a planet's surface. These were designed to help students learn basic geological features found on each planet. As they double-clicked on tour stops in the "Places" sidebar, they were flown to the location with a preset camera view and a balloon displayed a description of the location as well as an associated picture (a few contained a video clip or animated GIF). The students were able to roam and explore the surrounding area using the standard Google Earth navigation controls, which they were introduced to prior to the lab.

Google Earth comes with Mars and Earth's Moon virtual globe imagery built in. For Mercury and Venus, image overlays were created on top of the Earth terrain imagery (De Paor et al. (2012b)).

The PDF versions of the laboratory class consisted of identical content as seen in the KML tours albeit without the animated images and videos. The style was similar to that of a textbook with two columns and associated figures (Fig. 6). The students were asked to open the PDF, read through it on-screen, and discuss the content with their classmates. They were asked to take turns reading the PDF out loud.

Mercury

A virtual globe of Mercury is not built into Google Earth. The NASA MESSENGER Mission outreach site does include a downloadable KMZ file simulating Mercury on Google

Sample PDF Content
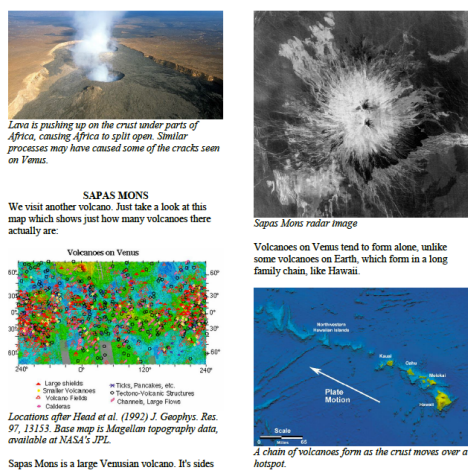
FIG. 7: Sample PDF content. Text and images were identical to the placemark balloons.

Earth (MESSENGER 2016). However, their tour contains almost 1,000 places of interest — many more than can be accommodated in an undergraduate or second level course. Also their KML code contains an error that causes the Earth's terrain imagery to poke through on zooming. This study created a more concise tour of key features of Mercury and overlaid it on Google Moon, which is much closer in size, does not have an atmosphere that has to be turned off, and does not show tropics and polar circles on its grid in the View menu.

Hovering above the surface, students first see that there is effectively no atmosphere on Mercury and they invariably note that the surface is quite similar to our Moon. In fact, instructors can challenge students to study the terrain and be able to tell whether they are looking at the Moon or Mercury. Students read about the dramatic difference in day and night temperatures, a consequence of Mercury's proximity to the Sun.

The presence of ice in permanently shaded polar craters is highlighted and is explained by the planet's lack of axial tilt. Students also learn about 3:2 spin-orbit resonance and view Mercury's huge core. The inner, middle, and outer cores are represented by huge 3-D COLLADA models. Students can also manipulate a COLLADA model of the magnetic field and its interaction with the Sun's field. In line with the classical European Grand Tour concept, the first tour stop on the surface is the Rembrandt Crater. Students then visit the Caloris Basin, including its faults and a volcano near its rim, and follow a video ground wave to the antipodal crumpled terrain, a consequence of the entire planet ringing like a bell as a result of Caloris Basin formation during the Late Heavy Bombardment 3.9 billion years ago.

Essential features of Mercury are the scarps called rupes resulting from rapid cooling and shrinkage after core mantle differentiation. A highlight of the tour is the large volcanic region that MESSENGER discovered near the North Pole. Finally, students return to a satellite view of the planet and review its geological history.

Venus

Google Venus is built on Google Earth, which is similar in size. Here, instructors need to check that students do not display Earth's atmosphere or latitude and longitude grid. A graticule was created for Venus which displays longitude from $0°$ to $360°$ east of the Prime Meridian and does not have tropics nor polar circles.

Hovering over Google Venus, students can compare and contrast the global features of Earth's so-called sister planet, including its bulk density, orbit, and spin. They view its atmosphere via an overlay and note the atmospheric super-rotation. Next, the atmospheric overlay is turned off to reveal NASA SARS imagery which is tiled over the surface. Placemarks point out the lack of an Earth-like division into land and sea, and the very different distribution of volcanic craters compared to Earth's mid-ocean ridges and volcanic arcs. The landscape is divided into Lowlands, Mesolands, and Highlands. Tour stops include Addams impact crater, with its melt apron, and pancake-like lava domes. Students zoom into two features unique to Venus, the Artemis Super-plume and the Ishtar Terrain. They should be encouraged to debate the possibilities for past plate tectonics and discuss the concept of recent resurfacing. The tour ends again with an overview from space, a view of large COLLADA models of the interior, and an account of the run-away greenhouse effect.

The Moon

The Grand Tour of Earth's moon is more detailed since more data is available from manned and unmanned missions and telescopic observations. Google Moon is built into Google Earth and users are prompted to switch to it when they load the KML file. The tour begins with the familiar view of the near side from space. Students note dimensions, phases, tidal locking, and eclipses, and the division of the surface into heavily cratered terrain and smoother maria. They view hand specimens and thin sections of basalt, anorthosite, breccia, orange soil, and a model of water ice distribution. The tour of geological structures includes Hadley Rille, linear and arcuate fractures, volcanic domes, and wrinkle ridges. Students visit Tranquility Base, the place where the Eagle landed and Neil Armstrong took a giant leap for mankind. The stop includes historic video of this event, which surprisingly some students

have not seen.

Students next compare the near and far sides of the Moon, visiting prominent craters and maria. They compare gravity anomaly maps and are challenged to discuss the Big Whack theory of lunar formation, the possibility of a coalescence of two protomoons, and the Nice model explanation of the Late Heavy Bombardment and subsequent mare formation (Gomes et al., 2005). The tour ends with the latest water ice data suggesting true polar wandering.

Mars

Mars is also treated with considerable detail thanks to the amount of orbiting and rover mission data available. To emphasize the difference in size of Mars and Earth, we created a semitransparent model of Earth's contents hovering high over the Martian surface and used the "extend to surface" feature to dramatize the scale difference. Students view historic maps built into Google Mars and visit 3-D models of its moons, Phobos and Deimos.

The tour addresses atmosphere and climate, surface features, rocks and outcrops, and the geophysics and geology of Mars. It is worth remembering that the current generation were young children when the NASA rovers first landed on Mars and may have a strong emotional connection to those exciting events. Tour stops include real surface imagery, dust devils, and a Martian sunset. Ending the tour, students are invited to discuss the possibilities for life on Mars and the probability that human life will reach the planet in current lifetimes.

1.5 DATA COLLECTION

Identical pre-, post-, and follow-up questionnaires for each planet were used to score student performance, and they were closely aligned with the content of the tours. The questions were designed to limit guessing and encourage critical thinking rather than memorization. For instance, the use of multiple correct answers, although difficult to score, was formulated to encourage reasoning skills.

Observations were also performed during the laboratory tours by recording in a notepad any interactions (or lack thereof) between the students and their tours. Additional details such as whether students finished earlier than expected or later, or whether any technical difficulties were experienced during the experiment were also recorded. We also developed an interview protocol to be employed with a subset of students in order to get their perspectives on the tours and what they learned through their interactive participation within the tours. The students who participated in the study were asked whether they would like to voluntarily participate in a follow-up interview. As a result of this process only three students were

Average Student Scores			
	Pre-test	Post-test	Follow-up
Whole class	36.1% ± 12%	46.7% ± 13%	42.9% ± 14%
Treatment (KML)	35% ± 13%	48.4% ± 12%	42.4% ± 13%
Comparison (PDF)	37.6% ± 12%	44.2% ± 14%	43.9% ± 14%
Change	statistically significant gain for GE versus PDF		not significant

TABLE 1: Table was generated using Microsoft Excel and gives the average of all student scores as percentages with the standard deviation for the pre-test, post-test and follow-up. Numbers were rounded to the nearest whole number.

interviewed.

1.6 DATA ANALYSIS

To score the pre-, post-, and follow-up tests, a scoring mechanism was needed. Two rubrics were designed: the M-Rubric for multiple-choice questions and the C-Rubric for critical thinking or short answer questions. The M-Rubric was also used for all multiple-choice questions with more than one correct answer. It is represented by the following equation,

$$r = \frac{-s}{(N-c)} \tag{1}$$

where, $r < 0$ and is the number of points reduced per wrong answer from the total points available (s) over the number of answer choices provided (N) minus the number of correct answers (c). Once r is obtained, the following equation can be used to calculate the final points assigned to a multiple-choice question:

$$\sum Q_R - \sum Q_W r = \phi \tag{2}$$

Here, Q_R is the number of correct answers, Q_W is the number of wrong answers, r is the number of points reduced per wrong answer, and ϕ is the final number of points awarded and is ≥ 0.

A C-Rubric was designed for all short answer and critical thinking questions. This consisted of points ranging from 0 to 3. If the student did not recall anything they saw in the tour or did not provide any reasoning, they received 0. If they demonstrated accurate and complete recollection, justification, and reasoning then they received a score of 3. Incomplete efforts scored 1 or 2. To be consistent, prior to grading questions which required

C-Rubric Example Questions

22. In what three ways is the climate of Mars similar to that of Earth?

0pts...................... Blank, I don't know, Aliens, did not answer the question
1pts...................... Seasonal changes/weather changes (gave one example)
2pts...................... Seasonal changes/weather changes (gave two examples)
3pts...................... Polar ice caps, seasonal changes, weather patterns, temperature with
location and time of year (gave three examples)

C-Rubric
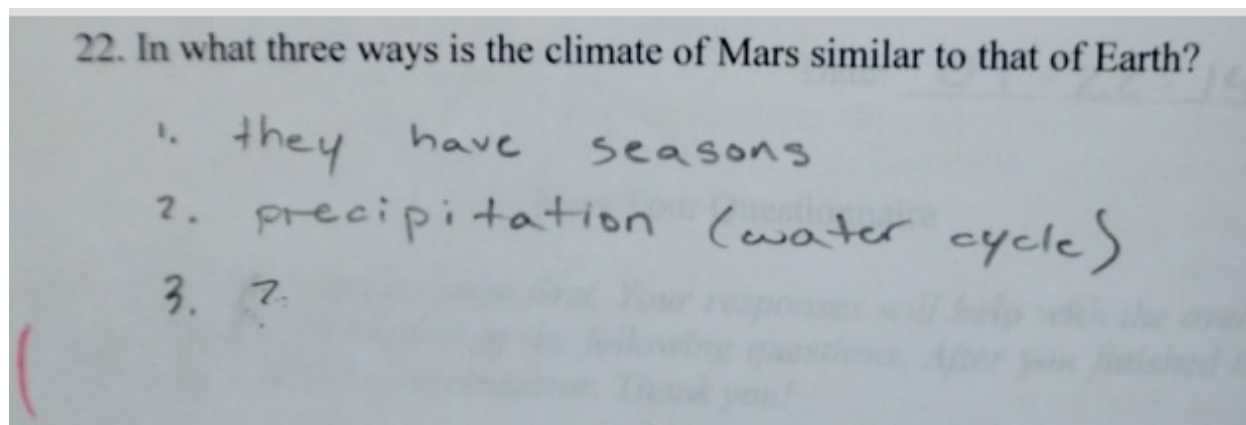
11. Why have craters on Mars remained more intact whereas craters on Earth have eroded?

Ans. Earth impact craters erode quickly from running water and oceans whereas on Mars there is currently no evidence for oceans or running water.

0 pts...................... left blank, "I don't know", rephrased the question, unrelated answer
1 pt......................"Because of the atmosphere", "More activity on Earth", "Plate tectonics don't move"
2pts......................Mentions water or plate tectonics but with other wrong answers
3pts......................"Earth has water and/or plate-tectonics, Mars does not", no water erosion
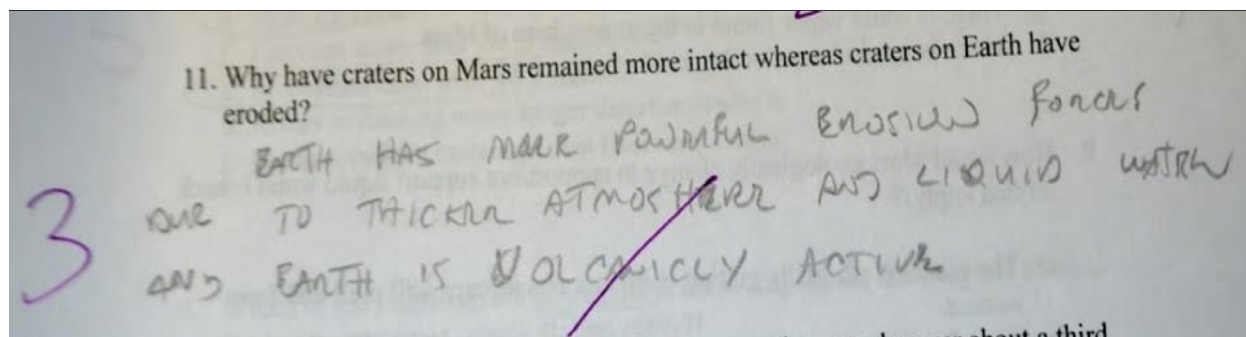
FIG. 8: Two examples of questions asked in the pre-test, post-test and follow-up that were scored using the C-Rubric and the corresponding student responses.

the C-Rubric, a sample of possible answers and their associated score ranging from 0 to 3 was created as a template. An example of how the C-Rubric is applied in this study is demonstrated in Fig. 8.

The C-Rubric was exclusively used to score short answer responses, which tried to test critical thinking. The C-Rubric was used by initially creating a template of ballpark answers and aligning responses accordingly when scoring, trying to minimize inconsistency as much as possible.

Using these two rubrics, each pre-, post-, and follow-up test was scored by the first author only (see supplemental files). Each planet and Moon was scored out of a total number of points which varied depending on the planet's total number of questions. A 2 (pre-test, post-test) × 2 (PDF, KML) Repeated Measures Analysis of Variance (ANOVA, Everitt, 2014), was used to test the short-term results. Before analyzing the data, students' test scores were converted into z scores to make the results for different planets comparable. A z-score is the number of standard deviations between a score and the mean of a set of scores, positive being above, negative below, and zero equal to the mean. We computed z scores for all students within each group (PDF, KML), and also screened the data for underlying assumptions of ANOVA (normal distribution, equality of variances, etc.) and found no significant violations of assumptions. To investigate long-term effects, we used a 3 (pre-test, post-test, follow-up) × 2 (PDF, KML) Repeated Measures ANOVA, which assessed change in test scores from pre-test to post-test to follow-up. After scoring, we processed data for each laboratory using the Statistical Package for Social Sciences (SPSS, 1990).

In addition to the ANOVA statistical analysis, Microsoft Excel was used to plot the students' average scores and standard deviations for the pre-, post-, and follow-up in Table 1. Excel plots were also created to examine the similarities and differences in student performance.

Observations of students who participated in the study were recorded on a notepad. Students were watched as they interacted with their given tour style. We unobtrusively noted how they behaved as individuals and groups. The student's apparent enthusiasm and focus on task were also noted. Results of observations were analyzed by reading through the written recordings and highlighting important key features.

Interviews with three participants were transcribed verbatim and analyzed using the computer program HyperResearch (Hesse-Biber & Dupuis, 2000). The first two authors examined the three interviews simultaneously and collectively identified 30 overarching themes within the data. This process relied on an inductive approach to data analysis whereby
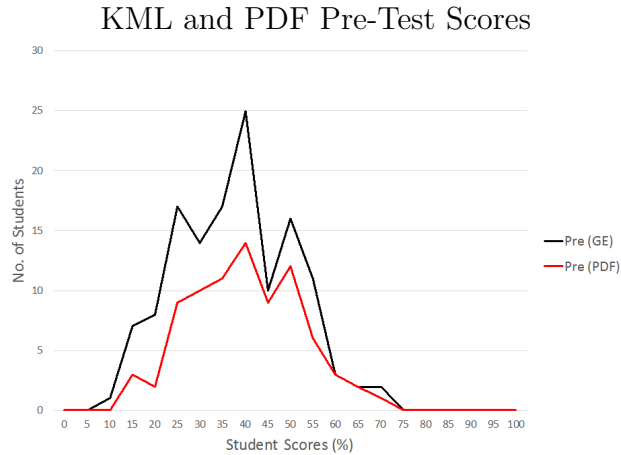
FIG. 9: Pre-test score comparisons of the KML (Google Earth) and PDF groups. The x-axis represents the students' scores as percentages, and the y-axis is the number of students who made up the group.

themes emerged from interviews and were constantly compared both within and among participants (Corbin & Strauss, 2008). The interviews were used to help understand reasons behind positive gains revealed through analysis of the questionnaires in addition to allowing the authors to develop an understanding of participant perspectives regarding the experience.

1.7 RESULTS

1.7.1 TESTING

When approximating the curves as "bell" curves, the PDF group's center is greater than the KML's center (Fig. 9). This indicates that the PDF students came into the tour with a slightly greater knowledge of the material than the KML group.

The post test histogram revealed that the majority of students, 25 in total, from the KML group (Google Earth users) obtained a score of 56 out of 100 (Fig 10), whereas the majority from the PDF ground, 13 in total, only scored as high as 45 out of 100. Similarly, the peak in the KML curve increased from 40% to 55%, whereas the peak in the PDF curve increased from 40% to 45%.

The pre-test and post-test can also be compared from each group individually (Fig. 11). For the KML (Google Earth) users, one can visually see from the plots that the majority has
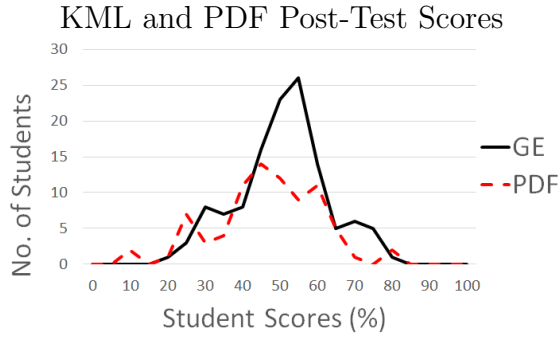
FIG. 10: Post-test score comparison of the KML (Google Earth) and PDF groups.
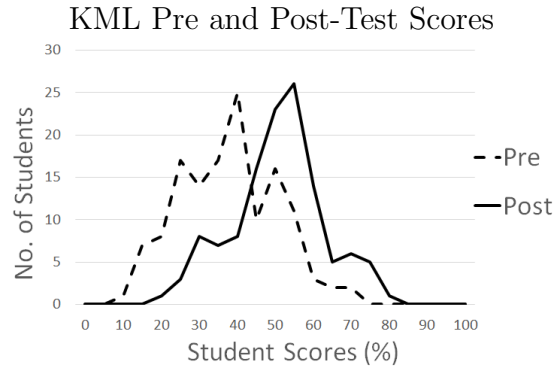
FIG. 11: Pre-test and post-test scores of treatment (KML, shown as Google Earth) group.

shifted to scoring higher after they participated in their tour. For the pre-test, the center of the asymmetric Gaussian is between scores 32-45 whereas after the tours the center falls between scores 45-60.
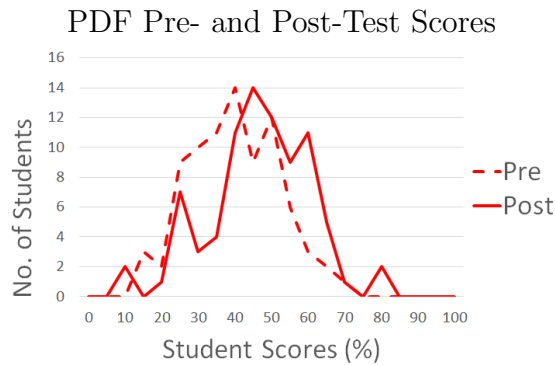
FIG. 12: Pre-test and post-test scores of comparison (PDF) group.
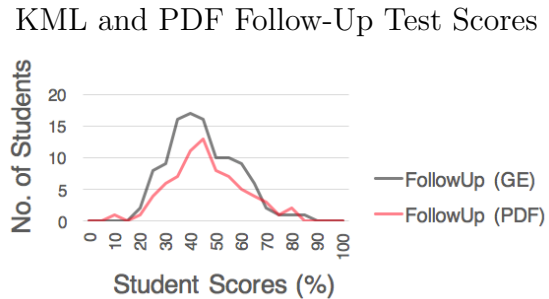
FIG. 13: Comparison of the follow-up test for the KML (Google Earth) and PDF groups.

For the PDF group, the shift is not as prominent (Fig 12).

Finally, for the follow-up test that was administered weeks later, the peak for the KML (Google Earth) group fell at a lower score than it did for the PDF group (Fig. 13). Again, the PDF group started with a higher background knowledge of the material covered in the test, and they retained that initial knowledge throughout the study.

When examining the post-test and follow up only in the KML (Google Earth users) group, it was apparent that the large number of students who scored highest (between 50-60%) in the post-test soon forgot what they learned weeks later after not having interacted

GE Post- and Follow-Up Test Scores
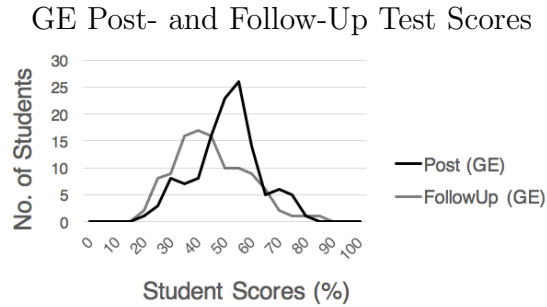
FIG. 14: Google Earth comparison of student scores for the post-test and follow-up test administered 11 weeks later.

PDF Post- and Follow-Up Test Scores
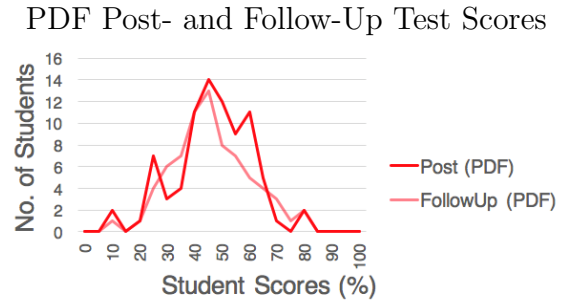
FIG. 15: PDF comparison of student scores for the post-test and follow-up test administered 11 weeks later.

with the tours (Fig. 14).

The graph in (Fig. 16) the deviation from the average score for all participants indicated for the two different groups (KML and PDF) in the three tests (pre-, post-, and follow-up). Both groups did better on immediate post-test, but KML (Google Earth) group did significantly better. Then both groups reverted on follow-up test. They were still better than their pre-test scores. Note that absolute performance is not shown, as it is not relevant.

Results indicate that in the post-test, the KML group scored higher than the class average score (indicated by a 0.00), and the PDF group scored lower than average, hence a negative value. This does not mean that a negative score was achieved, but just that the average PDF post-test score was below the average for all students. Specifically, there was a significant difference between the pre-and post-test ($p = 0.041$) but there was not a significant difference between the pre-test and follow-up test ($p = 0.069$) when comparing the PDF and KML groups. Results of the 2×2 multivariate repeated measures ANOVA indicated a significant multivariate interaction between time and treatment condition: Wilks's $\lambda = 0.98$, $F(1, 200) = 4.22$, $\eta^2 = 0.02$, $p < 0.05$ (e.g., Mardia et al., 1979). This interaction indicates that changes over time from pre- to post-test differed by condition. Specifically, the average score for the treatment group (KML) which interacted with the Google Earth tour improved from pre-to post-test ($M_{z\ score} < 0.01$, $M_{z\ score} = 0.13$, respectively) in relation to the entire population while the average score for the comparison group (PDF) decreased from pre-to post-test ($M_{z\ score} = 0.03$, $M_{z\ score} = -0.16$, respectively) in relation to the entire population. This means that the students who used Google Earth were, on average, 0.13 standard deviations above the average exam grade at post-test while the students who received PDF were -0.16 standard deviations below average on the post-test. It should be noted that both
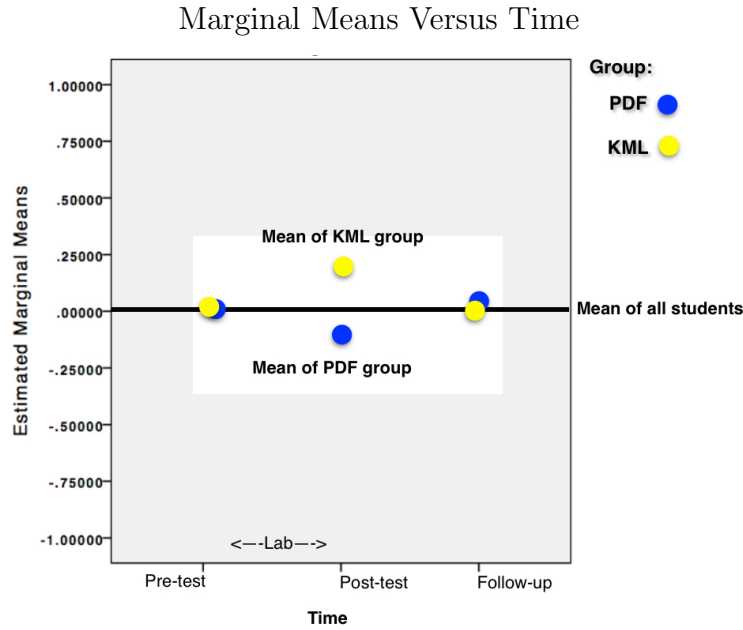
FIG. 16: Plot of estimated marginal means versus time.

KML and PDF groups demonstrated some modest gains from pre- to post-test, but that the post-test scores exhibited by the KML group were significantly higher on average than those from the PDF group (Fig. 17).

The KML group started out with less knowledge than the PDF group. The KML group out-performed the PDF students with the post-test. At the follow-up test, both groups forgot most of what they learned but still retained a decent amount more than they started with. It appeared as if the PDF did better at the follow-up however, one must take into account the huge jump in the KML pre-test to post-test in comparison to the jump seen from PDF pre-test to post-test.

The multivariate results for the time × condition interaction (pre-, post-, follow-up) were marginally significant: Wilks's $\lambda = 0.97$, $F(2, 164) = 2.71$, $\eta^2 = 0.03$, $p = 0.069$. While the linear within-subjects univariate test was non-significant ($F[1, 165] = .005$, $\eta^2 < 0.00$, $p = 0.945$), the quadratic interaction effect was significant ($F[1, 165] = 5.33$, $\eta^2 < 0.03$, $p < 0.05$). Specifically, the comparison (KML) increased in test z score from pre- to post-test, then decreased in test z score from post-test to follow-up while the treatment group decreased in test z score from pre- to post-test, then increased in test z score from post-test to follow-up. This suggests that the effect using Google Earth (KML) was short-term, since significant differences between the groups disappeared in the follow-up tests.

PDF Versus KML Group Averages
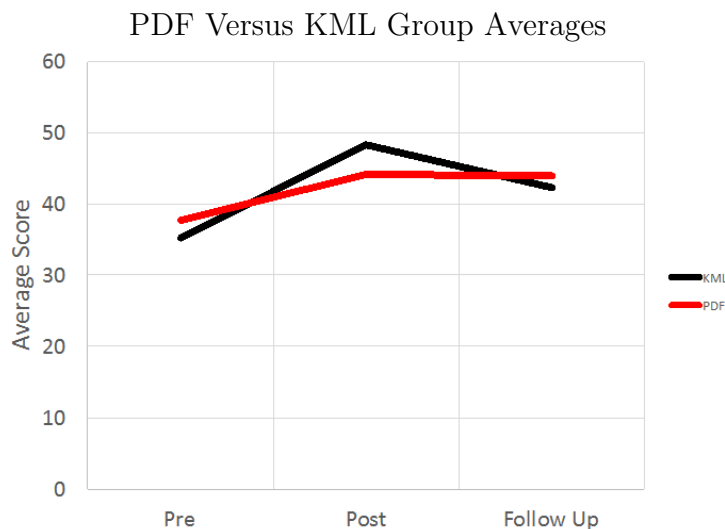
FIG. 17: Plot comparing the PDF and KML (labeled as Google Earth) group using average scores for pre-test, post-test, and follow-up.

1.7.2 OBSERVATIONS

Students were observed in action while they participated in the labs. Observations were almost entirely drawn from the back of the classroom, with occasional close-by monitoring. Detailed written recordings included striking impressions left by students during the laboratory period, such as student engagement or lack thereof. Most students using Google Earth appeared relatively engaged and conversational with their fellow group members while they explored each tour stop on their given planet. Very few groups in each class were disengaged from the material. Some started to explore other features on Google Earth. Some students who did not have control of a mouse glanced away from the screen. A few students asked their instructors questions about the status of current missions and discoveries on the given planet. One group explored beyond the given assignment, trailing off to other planets and exploring additional built-in features such as historical maps and layers for the planet Mars. Those students who were not familiar with Google Earth seemed initially overwhelmed and frustrated by the interface but they navigated smoothly after reading instructions and collaborating with group members.

Overall, students reading the PDF appeared relatively quiet for the entire duration of the tour. One PDF group asked, "All we are doing is reading?" Most students skimmed through the PDF paper and finished earlier than those who used Google Earth. PDF students displayed signs of boredom such as minimizing and maximizing the PDF window repeatedly

or randomly highlighting empty space on the document. One PDF group took turns reading the PDF out loud but quit halfway and read the remainder in silence. As one group member scrolled the text, group members glanced at the associated images or out into space. Group members who were verbal discussed topics unrelated to the assignment.

1.7.3 INTERVIEWS

In addition to testing, we conducted a few student interviews. **Students 1** and **2** read the PDF and **Student 3** followed the Google Earth tour. All three studied Mars. During the interview, **Student 2** hesitated to confirm which tour she participated in; vaguely claiming the tour was interactive where she zoomed to different tour stops. This was a student who was part of a treatment group where half the room read PDF's and the other side of the room used Google Earth. The students in this laboratory faced their backs to each other; however, occasional wandering of eyes, inspecting the screens of fellow classmates may have taken place.

1.7.4 POSITIVE RESPONSE TO VISUAL AIDS

All three students responded positively to any visual aides presented. As stated by **Student 1**: "I think that pictures made [the PDF document] more interesting. Had it been just words, I think I would have gotten maybe a little bored and not interested." **Student 1** also expressed more interest in wanting to participate in the Google Earth tour instead of reading the PDF, stating "I was just more disappointed that I didn't get the Google Earth" after being asked about her perception of the tour.

1.7.5 SELF-REPORTED KNOWLEDGE FROM TOURS

When asked what they learned, **Student 1** said she "learned about the moons and the craters" as well as the "type of rovers that have landed on it." She added that Mars is "more of a red color" with a "temperature hotter than most of [the other planets]," evidently confusing regolith color for black body radiation. She also said "there is a possibility that Mars may have had water on its surface due to the craters and the way it is shaped." **Student 2** said she learned that Mars is not an empty, smooth planet but filled with craters and volcanoes. **Student 3** said he learned about the "solar system's largest extinct volcano, Olympus Mons [and] the world's [sic.] deepest canyon, even bigger than the Grand Canyon,

Valles Marineris".

1.7.6 EFFECT OF TOURS ON STUDENT INTEREST

When each student was asked whether they were more interested in planetary science after the lab, **Student 3** said: "I'm more interested, especially when New Horizons gets to the ninth planet next year". This student was referring to NASA's spacecraft, which made history recently by taking close images of Pluto, the farthest terrestrial body photographed so far. The student seems to have an interest in planetary exploration, which according to him was further fueled from participation in the Google Earth tour.

Student 2 wanted to know "If it's like that on other planets. Like does it rain on Venus?" she asked. (It does in fact rain on Venus, however it rains sulfuric acid, not water, and that evaporates before reaching the surface).

1.7.7 STUDENT PREFERENCE OF TOUR TYPE

One of the most interesting comments came from Student 1 who was asked to expand on her idea that the PDF was more "educational" than the Google Earth tour. She responded as follows: "When I think of like words or anything like that, I just put education together. Because usually in school, that's what you have to do. In almost [all] your courses, they'll ask you to read an assignment and to maybe like answer the questions that follow. So I just kind of thought okay, this is something educational. I'm having to read an assignment and answer the questions. But a Google Earth assignment, I feel like that's more of an opportunity for you to maybe do something that isn't written down or something that isn't on the paper for you to do that day." When this student was asked which tour style she thought she would learn more from she said: "I think I'll probably learn more from the traditional version because there's more information that you don't know [there was in fact no difference in content]. But the Google Earth version is just more interesting, like a more interesting experience."

1.8 LIMITATIONS

There are factors which have likely effected the outcome of this study. For instance, training on the Google Earth interface and navigation system was insufficient. Ideally, students should train thoroughly beforehand. The Google Earth content balloons which appear

Mars Webpage
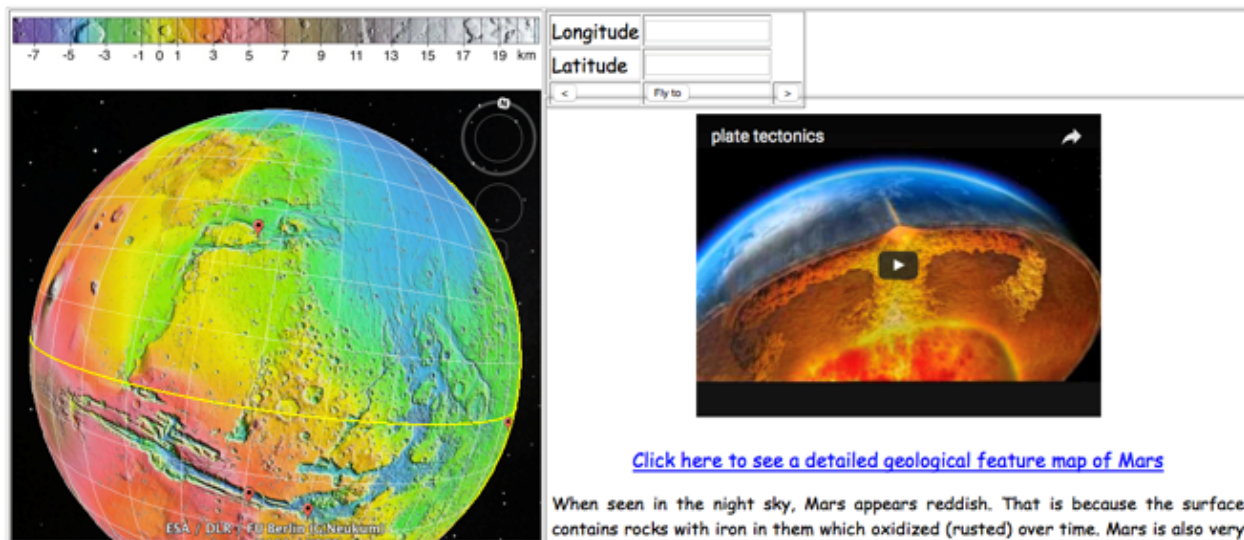
FIG. 18: The Mars webpage as an alternative to the Google Earth platform for simplistic lesson plans.

when the user clicks on each tour stop, provide useful information of each tour stop. However, they inconveniently display in front of the tour stop location, thus blocking it from view. The student either has to manually close the balloon in order to read the content, or click anywhere on the planet, and the balloon content window closes automatically. A more organized way of presenting the material would be to have students roam around the planet at the same time as viewing the information balloon which describes what they are looking at. This style of interface has already been designed for Mars, as a webpage (Fig. 18). The Google Earth interface has been placed on the left of the webpage and balloon boxes open up on the right side.

The study was carried out in a single week of a semester-long course. Were Google Earth to be used in successive labs, students would become more familiar with navigation and might retain more knowledge long-term.

Students were told that they would receive 100% credit for participation regardless of performance (a requirement of IRB compliance). They might have retained more long-term gains if their grade were at stake and perhaps put in more effort in their answers.

Students were overwhelmingly non-science majors. There might be a significant difference in motivation for science majors, especially geoscientists.

Finally, groups of three students shared one computer. Learning outcomes might have been different for student pairs or solo students. It was noted via observation that often one student took control of the mouse which left the other two members disengaged.

1.9 CONCLUSION

Instructors can easily overestimate the technical savvy of students. Despite being the digital device generation, and despite their expertise in communicating via Facebook or Twitter, students need lots of help with very basic aspects of apps such as Google Earth. To mitigate this issue, a detailed set of navigational instructions was provided to both KML and PDF groups prior to their lab, however the struggles students had with navigation suggest that few bothered to prepare.

The results of our study revealed modest short-term gains on the post-questionnaire for the KML (treatment) group that were significantly higher than gains exhibited by the PDF (comparison) group. This indicates a significant impact on the knowledge of students who followed a tour on an interactive virtual globe. Therefore, it is recommended that instructors provide opportunities for such active learning. However, long-term learning gains vis-a-vis the treatment group were not maintained. While the Google Earth treatment was initially more effective than the PDF experience, students soon forgot what they learned. A one-shot treatment is therefore not sufficient. Perhaps continued active learning opportunities would have yielded more lasting results. This is a proposition worthy of future investigation. In the meantime, it is suggested that instructors facilitate ubiquitous learning outside of fixed laboratory periods in order for students to review material throughout a semester long course and provide incentives for students to become familiar with controls (or penalties for failing to do so).

Virtual globes such as Google Earth can help educators bring lesson plans to life by allowing students to actively explore but more work is needed to ensure long-term benefits.

CHAPTER 2

TESTING FOR CONVECTION IN THE UPPER MANTLE OF MARS

2.1 INTRODUCTION

2.1.1 MOTIVATION

Stagnant Lid Versus Active Lid Convection
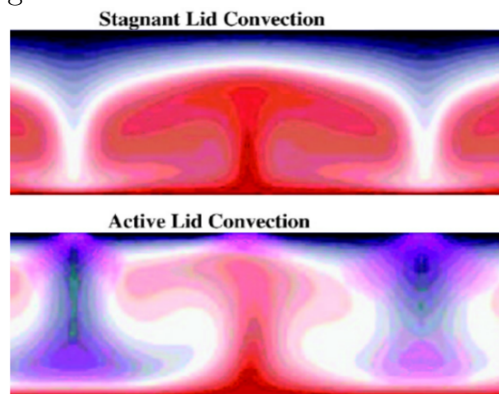
FIG. 19: Top image shows a thick, non-interacting lithospheric lid and convection currents underneath and represents the upper mantle of Mars. Bottom image shows convection currents reaching the lithosphere. Images taken from Robin et al. (2007).

The objective of this investigation is to determine conditions, if any, that will give rise to plate-tectonic-like processes on a Mars-sized planet. The research addresses the question, "could a Mars-sized planet ever have had vigorous upper mantle convection, and would it be consistent with plate tectonic processes?" This study uses a simple exploratory model to investigate convection of a thermally buoyant fluid with properties that are representative of mantle material. Given the right conditions, the model may predict plate-like structures that will sink since they are denser than the underlying material. This is similar to the subduction processes on Earth, where the lithospheric plates converge. It is believed that Earth evolved from stagnant lid convection (Fig. 19) to plate tectonics (O'Neill et al., 2016).

Mars, in its current stagnant lid mode, may be a window into earlier Earth, and maybe future Earth.

2.1.2 STRUCTURE OF A TERRESTRIAL PLANET
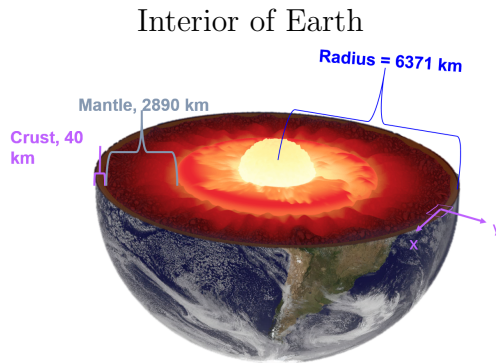
Interior of Earth

FIG. 20: Interior of Earth showing its solid inner core, liquid outer core, mantle, and crust.
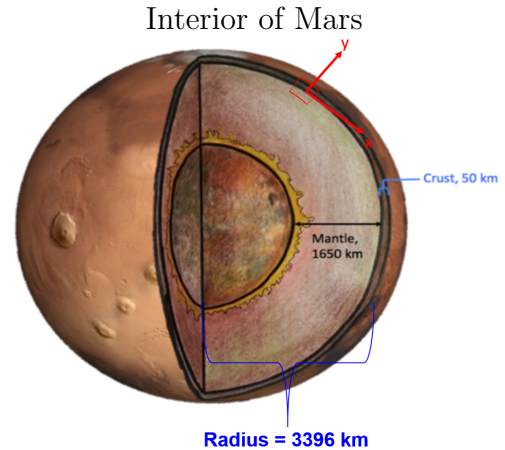
Interior of Mars

FIG. 21: Interior of Mars showing its liquid core (Stewart et al., 2007), depicted as a yellow jagged layer, along with estimated mantle and crustal (Zuber, 2001). Illustration interior by F. Coba.

Mars is about half the radius of Earth and its surface gravity is 3.7 m/s^2, about 38% the strength of Earth's surface gravity. Like Earth, shown in Fig. 20, and the other terrestrial planets, there is evidence from the Mars Global Surveyor's thermal emission spectrometer data that the interior of Mars (Fig. 21) consists of an outer shell called the crust, an underlying mantle, and a central core (Zuber, 2001). Crust, mantle, and core are layers that resulted from gravitational and radioactive heating, and subsequent differentiation of a planet. The chondritic (young) Earth heated from radioactive decay, reducing the viscosity of denser metallic materials, and allowing them to sink into the core. Less dense stony/rocky material remained in the mantle, and continued to heat the planet. Thus, the density of the central core is much greater than that of the mantle. The crust, mantle, and core define the chemical layering of a planet, and are useful when discussing the compositional changes as a function of depth below the surface.

A second way of describing the internal structure of a terrestrial planet uses mechanical, rather than chemical, layer properties. The lithosphere is the cool, outermost, rigid shell of a planet, similar to the skin on a creme brûlée, and it includes part of the upper mantle. Below

Layers of the Interior of Earth
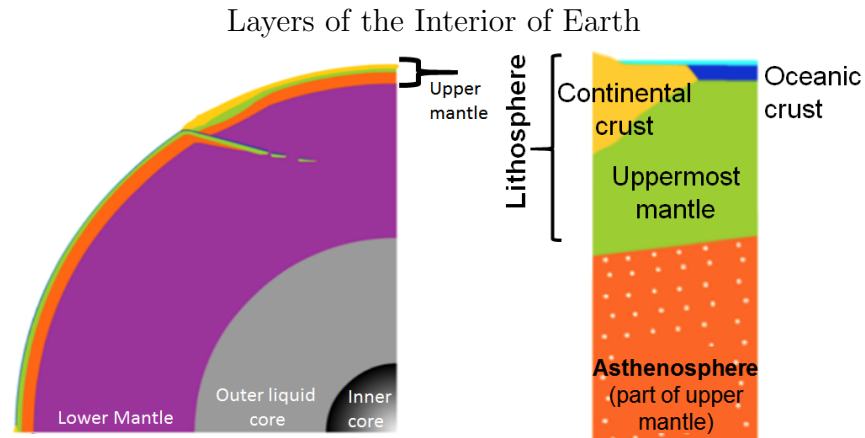
FIG. 22: Interior can also be divided by mechanical properties: upper mantle, lower mantle, outer core, and inner core. The lithosphere contains the continental crust, the oceanic crust, and the uppermost mantle. Illustration by D. De Paor

the lithosphere lies the asthenosphere. This is a region with viscosity, a fluid's resistance to flow, of 10^{19} to 10^{21} Pa s (Breuer & Spohn, 2006), about 100 times less than that of the lower mantle (Zuber, 2001). The asthenosphere is shown as purple in Fig. 22. For Mars, there is no direct evidence that there is currently an asthenosphere; however modeling of mantle convection on Mars requires its existence (Zhong & Zuber, 2001). The remaining layers inside Earth (Fig. 22) include the lower mantle, liquid outer core, and solid inner core. According to models by Rivoldini et al. (2011), Mars contains a liquid core. Genova et al. (2016) analyzed recent NASA gravity maps, and suggested that Mars has a liquid outer core. Whether the planet has a solid inner core is still uncertain.

Comparing seismic wave propagation through the Earth to the seismic data from Mars Viking 2 lander, (Anderson et al., 1977) concluded that Earth has a thinner crust than Mars, but a thicker mantle and core (Table 2). This is consistent with the fact that Mars is significantly smaller, and cooled faster as a result (Zuber, 2001).

Fig. 23 shows that the Martian crust is about 80 km near the Tharsis bulge. The Tharsis region appears as a white area on Fig. 23, and it includes the three volcanoes of Arsia Mons, Pavonis Mons, and Acraeus Mons as well as part of Valles Marineris, a deep canyon. The Martian dichotomy, or the visible division of elevation between the smooth plains in the northern lowlands and cratered southern highlands, is also visible in Fig. 23. How the dichotomy originated remains uncertain. One hypothesis is that plates in the northern hemisphere subducted under the southern hemisphere (Sleep, 1994). The northern lowlands

Average Physical Characteristics of Earth and Mars

	Earth	Mars	Units
Total radius	6370	3396	km
Crustal thickness	40	60	km
Mantle thickness	2900	1650	km
Core thickness	3470	1690	km
Mantle temperature	1350	$\sim$540	°C
Mantle viscosity	10^{19-21}	10^{19-21}	Pa s
Avg. magnetic field strength	50	< 1.5	μT
Gravitational acceleration	9.8	3.7	m s^{-2}

TABLE 2: Physical comparison of Earth and Mars parameters. Average physical characteristics of Earth and there is significant variability associated with some of these parameters. Mars has a thicker crust than Earth but a thinner mantle. This is due to Mars' smaller size, which allowed the planet to cool faster (Turcotte & Schubert, 2002; Zuber, 2001).

therefore were a result of seafloor spreading where the dichotomy boundary represents the plate margins (Watters et al., 2007). However, there is no geologic evidence of subduction along the dichotomy (Watters et al., 2007) such as in Arabia Terra (McGill, 2000). Another hypothesis suggested that vigorous mantle convection caused upwellings that melted and thinned the lithosphere in the northern hemisphere (Lingenfelter & Schubert, 1973). Similarly, a super-plume (a single upwelling of hot mantle rock) could have caused melting, which may have contributed to the formation of the crustal dichotomy (Ke & Solomatov, 2006). Numerical simulations from Leone et al. (2014) suggest that a giant impact melted and heated the southern hemisphere, resulting in the southern highlands. Subsequently, this created the volcanism in the southern highlands and suppressed the volcanism in the northern lowlands.

To date, most Mars missions have focused on the exterior surface features of the planet. In May of 2018, NASA plans to launch and place a robotic lander called InSight on the surface of Mars to study its deep interior (NASA, 2015). InSight stands for Interior Exploration using Seismic Investigations, Geodesy and Heat Transport. The lander will use a seismometer and a heat-flow probe (NASA, 2015) to drill beneath the surface of the planet, and it will provide additional information on the internal structure, constraining geophysical parameters such as crustal thickness.

Like crustal thickness, lithospheric thickness varies as a function of geologic setting on a planet, but the average thickness for old oceanic lithosphere on Earth is about 100 km. Earth's lithosphere is broken into approximately twelve major tectonic plates. The Martian
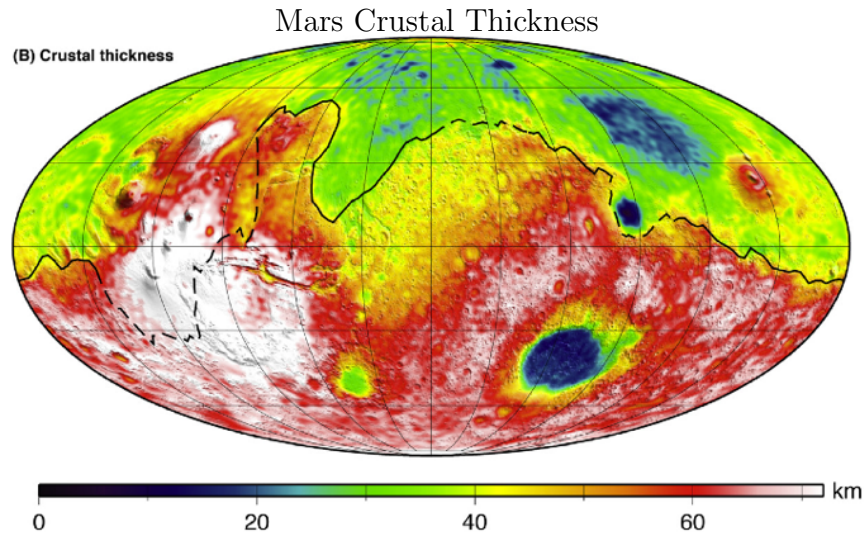
FIG. 23: (Image from Genova et al., 2016) Mars crustal thickness overlain on shaded topography. North is at the top, and west is left. The Tharsis bulge is on the lower left along with Olympus Mons and Valles Marineris. The white color represents the thickest crust whereas the blue is the thinnest crust. The crustal dichotomy is clearly visible as the division between thin crust (blue-green) and thick crust (white-red). The data come from Mars Reconnaissance Orbiter, Mars Global Surveyor, and Mars Odyssey.

lithosphere is a single plate. The average thickness is estimated to be between 150 km (Genova et al., 2016) and 300 km (Kiefer & Li, 2009).

2.1.3 PLATE TECTONICS ON EARTH

According to the theory of plate tectonics, the lithosphere of the Earth is divided into discrete rigid plates, which move at velocities of about tens of millimeters per year. The motion of a single plate affects that of the others. Wegener (1922) postulated that the continents used to be merged in a supercontinent called Pangea and that they "drifted" apart approximately 200 million years ago. He could not explain the cause of their motion though. Holmes (1931) hypothesized that thermal convection may be a possible driving force for the motion of the mantle on Earth. If the mantle is heated from within and cooled from above in the presence of a gravitational field, it becomes gravitationally unstable. Thermal convection can occur as the colder rocks descend into the mantle and the hotter, buoyant rocks ascend toward the surface. The Earth's mantle is heated from the decay of radioactive isotopes and from primordial heat remaining from planetary formation.

Illustration of Subduction
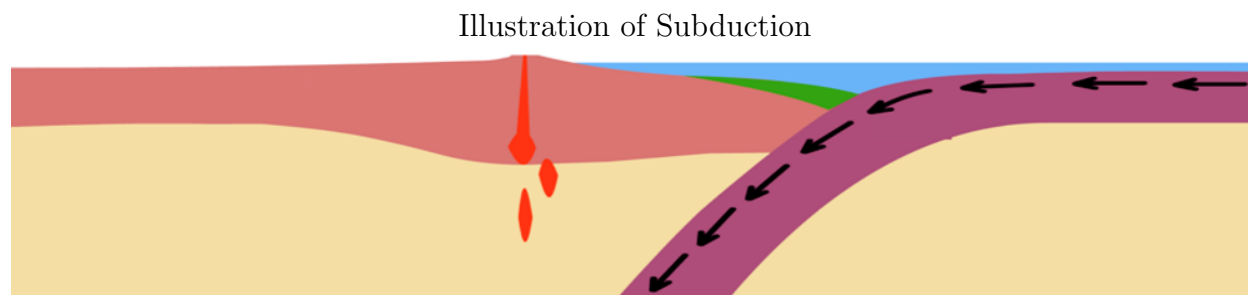
FIG. 24: Illustration of oceanic crust subducting under continental crust on Earth (De Paor et al., 2012a).

Gravity is the predominant force driving Earth's tectonic processes, acting on layers with contrasting densities (De Jong & Scholtan, 1973). Over time, the lithosphere becomes cooler as the planet loses heat. As rocks become cooler, they also become denser due to thermal contraction. Cold lithosphere is gravitationally unstable because the layer underneath the lithosphere is less dense and warmer. Because of negative buoyancy, the lithosphere bends and sinks into the interior of the Earth (Fig. 24) at subduction zones.

The downward gravitational body force on the descending lithosphere plays an important role in driving plate tectonics. The lithosphere acts as an elastic plate that transmits large stresses without significant internal deformation. The gravitational body force can be transmitted directly to the surface portion of the plate; this force pulls the plate toward the trench. This body force is known as slab pull. It has been calculated that slab-related forces account for 80-90% of the driving forces of plate tectonics (Conrad & Lithgow-Bertelloni, 2002).

University textbook sometimes imply that plate tectonics is driven primarily by forces that push the plates apart at mid-ocean ridges. In fact, ridge push accounts for a maximum of 10% (Conrad & Lithgow-Bertelloni, 2002). At a mid-ocean ridge, two plates are diverging, upwelling mantle material partially melts, and lava fills in the crack that is created. When lava encounters ocean water, it cools down to become basaltic ocean crust. The underlying asthenosphere becomes cooler and denser over time, causing the oceanic lithosphere to thicken and the seafloor to subside. This is the large negative density anomaly associated with a subducting plate. What happens to the subducting slab as it goes down into the mantle is still an open problem that is being investigated through seismic tomography, numerical modeling, and other geophysical studies.

2.1.4 PLATE TECTONICS ON MARS

Earth is the only terrestrial planet on which there is known plate tectonic activity. There are some indications from the Mars Global Surveyor of past plate tectonics on Mars (Zuber, 2001) in the form of tectonic ridges (Head et al., 2002) present in the northern lowlands. Having heated and cooled faster due to its smaller size, if Mars ever had plate tectonics, the plates would have become thicker than Earth's. Thicker plates require more strength to break and induce motion. This is consistent with the apparent lack of plate boundaries on Mars. The mantle of Mars obeys what is called the "stagnant lid" (upper stagnant layer on top of a convection layer) mode of heat transfer (Breuer & Spohn, 2006), and is believed to have done so for the majority of its existence. Convection is thought to occur on Mars today, with an absence of lithospheric motion. Evidence for current convection on Mars includes a volcano on Tharsis, which has been active in the last 10-30 million years (Sekhar & King, 2014).

2.1.5 FLUID MECHANICS

Models of mantle convection often treat asthenospheric rock, which is under high temperature and pressure, as a viscous fluid. Generally, fluids exhibit a frictional resistance to motion. The fluid behavior of the mantle was first established quantitatively by Haskell (1935) by approximating the viscosity to be about 10^{21} Pa s.

The Navier-Stokes equations are derived from Newton's Second Law and govern the motion of fluids. They are used in this investigation to calculate the motion of the mantle in the numerical model domain. For the case of incompressible flow, the density within the fluid parcel is constant, and the divergence of the velocity is zero. The equations conservation of momentum (Equation 3), energy (Equation 4), and mass (Equation 5) are given by:

$$(\vec{u} \cdot \nabla)\vec{u} = -\nabla p + \frac{\mu}{\rho_0 u_s L} \nabla \cdot \left(\nabla \vec{u} + (\nabla \vec{u})^T \right)$$
$$+ \frac{\vec{g} \beta L}{u_s^2} \left(T(T_c - T_h) \right), \tag{3}$$

$$\frac{dT}{dt} = \kappa \nabla^2 T - \vec{u} \cdot \nabla T + \frac{A}{\kappa}, \tag{4}$$

$$\nabla \cdot \vec{u} = 0. \tag{5}$$

Equation 3 equates inertial forces to pressure forces plus viscous forces and thermal buoyancy, where $\vec{u}$ is the velocity of the fluid, p is the pressure of the fluid, μ is the fluid dynamic

viscosity, T_c is the cold temperature, and T_h is the hot temperature. All of the other constants are defined in Table 3. Equation 3 uses the Boussinesq approximation, which ignores any small density changes across the fluid with respect to the reference mantle density, except in the buoyancy (body force) term, where is it multiplied by g, the acceleration due to gravity. Equation 4 is called the convection-diffusion heat equation. For this equation, T is the temperature, κ is the thermal diffusivity, and A is heat from radioactive decay. The heat equation describes how temperature changes in the mantle at a given time and location (dT/dt) depending on how the heat (energy) moves through the rock ($\kappa\nabla^2 T$), and how the rock physically transports this energy ($\vec{u}\cdot\nabla T$), along with any additional heat sources (A/κ). Equation 5 is the conservation of mass equation for an incompressible fluid, which says that the mass of the fluid is not created or destroyed.

In addition to the Navier-Stokes equations, it is also necessary to calculate the following dimensionless parameters:

$$\text{Ra} = \frac{\rho_0 \beta g L^3 (T_c - T_h)}{\kappa \mu_0}, \tag{6}$$

$$\text{Pr} = \frac{\mu_0 C_P}{k}, \tag{7}$$

$$\text{Re} = \frac{u_s L}{\nu}. \tag{8}$$

The Rayleigh number (Equation 6) is the ratio of buoyant (inertial) to viscous forces, and it determines the strength of convection. Thus, mantle dynamics are controlled by this parameter (Schubert et al., 2001, and references therein). The minimum Rayleigh number necessary for convection to occur, or R_{cr}, is on the order of 1000 (Koschmieder, 1993; Schubert & Anderson, 1985). The Prandtl number (Equation 7) gives the ratio of energy transfer by fluid convection to heat conduction. The Reynolds number (Equation 8) represents the ratio of momentum forces to viscous forces. It characterizes whether a flow is laminar or turbulent. Low Reynolds number indicates the fluid is approaching laminar flow, i.e. the fluid travels uniformly along a continuous path (streamline), and there is no mixing or vortices. Laminar flow occurs when the ratio of inertial to viscous forces is low. Creeping flow is a type of laminar flow, used when the Reynolds number for a fluid is much less than 1. All the variables found in all of these equations are represented in Table 3.

β is the thermal expansion coefficient of the material, which affects the buoyancy force. The heat capacity, C_P, is the amount of energy required to raise the temperature of the material by 1 K. The thermal diffusivity, κ, describes how well the material transmits energy

$$\underline{\text{Model Parameters for Mars}}$$

Variable	Meaning	Value	Units	Ref
β	Coefficient of thermal expansion	3×10^{-5}	$°C^{-1}$	Zhong & Zuber (2001)
C_p	Mantle heat capacity	1142	J kg^{-1} $°C^{-1}$	
g	Gravitational acceleration	3.7	m s^{-2}	
κ	Thermal diffusivity	1	mm^2 s^{-1}	Zhong & Zuber (2001)
k	Thermal conductivity	4	W m^{-1} $°C^{-1}$	
L	Length of the wall	400	km	
ρ_0	Reference mantle density	3440	kg m^{-3}	Goettel (1981)
Pr	Prandtl Number	2.855×10^{21}	unit-less	
Ra	Rayleigh Number	4×10^6	unit-less	
Re	Reynolds Number	1.85×10^{-20}	unit-less	
$T_\oplus$	Reference mantle temperature	1350	$°C$	
T_C	Temperature of top boundary	0	$°C$	
T_h	Temperature of bottom boundary	$0.4T_\oplus$	$°C$	
μ	Dynamic viscosity	10^{19}	Pa s	Breuer & Spohn (2006)
ν	Kinematic viscosity	2.91×10^{15}	m^2 s^{-1}	
u_s	Velocity Scaling Factor	2.3×10^{19}	cm yr^{-1}	

TABLE 3: Complete model parameters for the Martian mantle and their associated values and references.

through conduction relative to its ability to store heat. The thermal conductivity, k, denotes how quickly heat is transferred via conduction within a medium. The dynamic viscosity, μ, is the resistance of the fluid to deformations and shearing. The kinetic viscosity, ν, is the dynamic viscosity divided by the density.

2.2 COMPUTATIONAL MODELING FOR MARS

2.2.1 BACKGROUND

Schubert & Anderson (1985) provide a simple case for a viscous fluid with very high Rayleigh number and infinite Prandtl number, by analyzing the problem of 2-D thermal convection in a square domain with impermeable walls. They assume a Boussinesq fluid with constant properties such as viscosity. They ignore inertial forces, and use a finite element method. They simulated bottom heated mantle convection with Rayleigh number up to 10^5 times R_{cr}. Examples of their results are shown in Figs. 25 and 26, where they calculate single and double convection cell patterns (Fig. 25) and mantle isotherms (Fig. 26).

Thermal convection in the Earth's mantle has been modeled in many subsequent studies.

Fluid Motion in Convection Cells
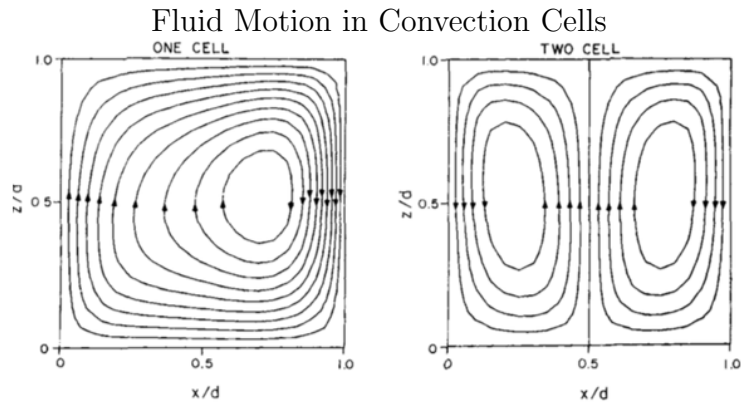
FIG. 25: Streamlines follow the fluid as it moves. Visible are one (left) and two (right) convection cells (Schubert & Anderson, 1985).

Isothermal Contours in Convection Cells
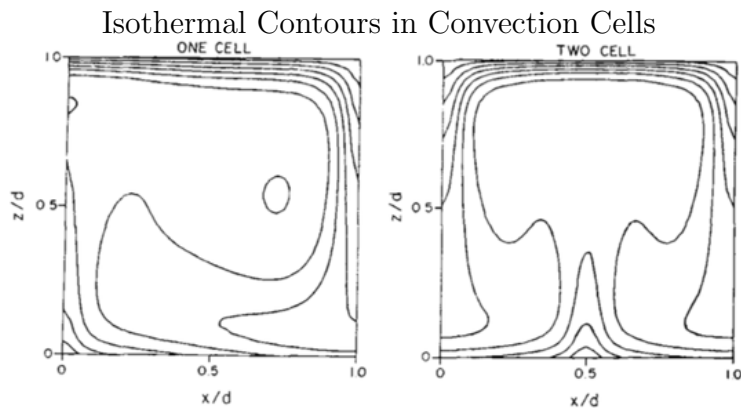
FIG. 26: Isothermal contours shows the temperature structure for the respective situations shown in Fig. 25, e.g., the two cell convection shows a plume structure (Schubert & Anderson, 1985).

For example, (Herein & Galsa, 2011) investigated time dependent mantle convection using COMSOL Multiphysics, the same software used in this thesis. In their study, it was found that the results from the cylindrical-shell geometry most closely matched three-dimensional modeling for convection. At high Rayleigh number of the mantle flow was time dependent and chaotic.

In a 2-D convection study of the entire Martian mantle, Zhong & Zuber (2001) found that there is vigorous convection in the first approximately 100 million years of Martian history, which may help explain the crustal dichotomy. Other investigations of Mars mantle

Simulated Temperature of Mars' Interior
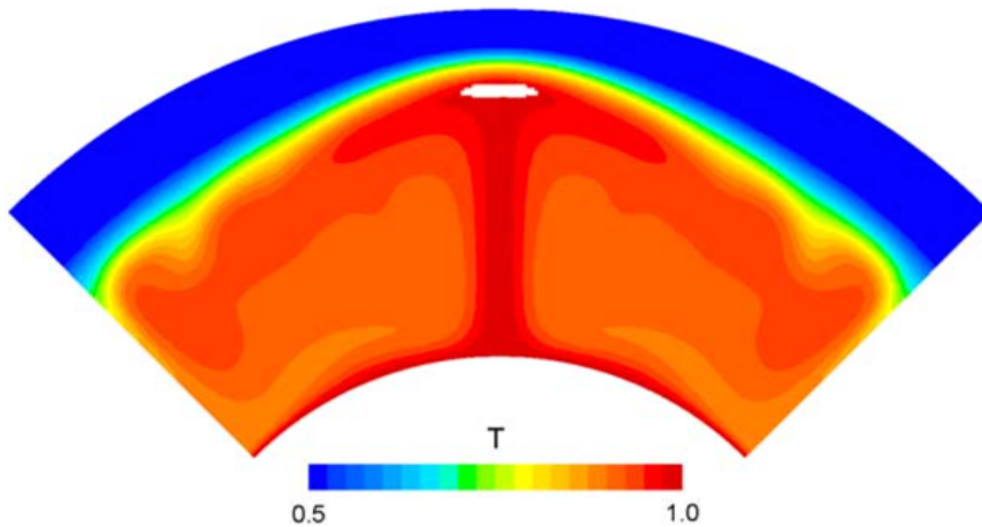
FIG. 27: Non-dimensional temperature plot showing a plume (Li & Kiefer, 2007).

convection (e.g., Kiefer & Li, 2009; Li & Kiefer, 2007) used a 2-D circular shell model domain of 1/8 of full circle, where the top surface was cold and bottom side was hot (Fig. 27). This study modeled plumes in a stagnant lid convection regime that lasted billions of years.

Sekhar & King (2014) investigated Martian mantle convection in a 3-D spherical shell, which produced multiple plume structures. They concluded that decreasing the Rayleigh number increased the lithospheric thickness, which increased the mantle temperature.

2.2.2 MODELING METHODOLOGY

The model used in this investigation simulated natural convection in the Martian mantle, which behaved like a slow-moving fluid with Reynolds number much less than one. Subsequently, creeping flow physics was used to calculate the fluid motion along with a Boussinesq approximation. A non-dimensionalized body force of $(Ra/Pr)(T-T_c)$ in the vertical direction drove motion within the model domain.

The model geometry is a hybrid of Schubert & Anderson (1985) and a classic corner flow model (Reid & Jackson, 2001) for Earth-like upper mantle convection. Corner flow models are widely used to represent the dynamics of the upper mantle of Earth. Corner flow models are driven by two mechanisms, buoyant upwelling and lateral motions of tectonic plates, and they do not include the motions caused by subducting plates. Corner flow models span the asthenosphere and the lithosphere at a mid-ocean ridge, where the lithospheric plates diverge

due to plate tectonics. Consequently, the corner flow model requires a moving top layer to simulate the natural tectonic nature of present day Earth. For Mars, lateral movements or shearing forces do not exist, only buoyancy-driven flow. Thus, as described in more detail below, there is no lateral plate velocity assigned to the top of the model domain in this investigation.

This work uses finite element model software COMSOL Multiphysics (version 5.1), available through the High Performance Computing at Old Dominion University. Initial steps followed the tutorial for "Buoyancy Flow in Free Fluids" available online from COMSOL. The tutorial is based on the work by de Vahl Davis & Jones (1983) who modeled steady-state natural convection in a square cavity for an incompressible fluid with a Boussinesq approximation. Their model, as explained in the tutorial, assigns different temperatures to the sides of the square, where $T_h = 1$ is the hot temperature, $T_c = 0$ is the cold temperature, and g is gravity. In the tutorial, none of the walls of the square domain are moving, only the fluid inside. The fluid is not able to penetrate out of the walls. Also, no-slip boundary conditions are used, where there is frictional coupling between the fluid and the walls at the domain boundary.

The tutorial model calculated fluid velocities and temperatures for Rayleigh numbers ranging from 10 to 10^6, for a given fluid with Pr = 0.71. However, for the purposes of this study, COMSOL was programmed to solve Rayleigh numbers ranging from 10 to 10^5 and only the 10^5 solutions are presented in the Results section. As shown in Equation 6, the Rayleigh number depends on gravity, and COMSOL solves the model for different Rayleigh values, indirectly changing gravity. The other parameter values, such as the Prandtl number, are fixed (Table 4).

The tutorial model was then modified for more Earth-like conditions. A temperature boundary condition of $T_h = 1$ was assigned to the bottom and the right sides of the square (Fig. 28), to be consistent with corner flow models. Temperature gradients across the model domain drive the buoyant flow that is responsible for natural convection. The left side of the square was insulated. Wall boundary conditions were changed from no-slip to free-slip. The Prandtl number was changed to 10^{25} (Table 4; see Appendix 2.5 for derivation). The Rayleigh number was set to 10^5. Mantle material was treated as a viscous Newtonian fluid where the stress in the fluid is linearly proportional to the rate of strain. The model had approximately 42,000 degrees of freedom, which can be thought of as the number of nodes multiplied by the number of fundamental problem variables (e.g., temperature, velocity) calculated at each node.
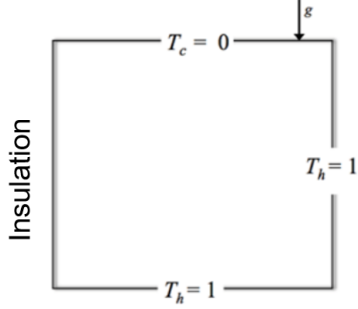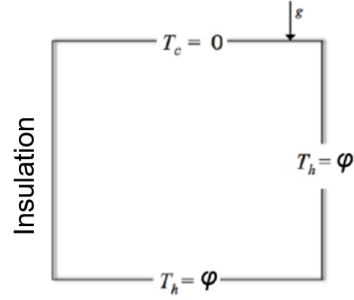
Boundary Conditions for Earth-Like Model

Boundary Conditions for Mars-Like Model

Earth-like model

FIG. 28: Earth-like model with square domain and boundary conditions.

Mars-like model

FIG. 29: Mars-like model with square domain and boundary conditions. Here ϕ indicates the ratio of the Mars thermal gradient to the Earth geothermal gradient.

Model Parameters Used		
Name	Value	Description
T_c	0	Top side temperature for Earth and Mars model
$T\oplus$	1	Bottom and right side temperature for Earth model
Pr	10^{25}	Prandtl number for Earth model
Pr	2.855×10^{21}	Prandtl number for Mars model
Ra	10^5	Rayleigh number at solution for Mars and Earth

TABLE 4: Non-dimensional temperatures and Prandtl number for the Earth-like model. After calculations, the temperature was scaled by 1350 °C. For Mars, the only change was the use of a Prandtl number equal to 2.855×10^{21}.

Next, a series of models based on the Earth-like model were used to investigate Mars-like mantle convection (Fig. 29). There were two differences between the Earth-like model and the Mars-like models. First, the Prandtl number was changed to $\sim 10^{21}$ (see Appendix 2.5 for derivation). Second, the temperature boundary conditions were modified to reflect cooler upper mantle temperatures in Mars as compared to Earth.

A thermal, or geothermal, gradient refers to the temperature increase per unit depth into a planet. The average geothermal gradient of Earth is between 20 to 25 °C /km (Fridleifsson et al., 2008), and the average Martian thermal gradient is between 10 to 15 °C/km (Ruiz et al., 2006; Solomon & Head, 1989). Therefore, for the Mars-like model, the bottom and right temperatures were set to $T_h = 0.4$, where 0.4 is the ratio of the geothermal gradient

on Earth and thermal gradient on Mars. Models were also run for a range of boundary condition temperatures in increments of 0.05 from $T_h = 0.35$ to $T_h = 0.95$, approaching the temperature of the Earth. By increasing the temperature, the model was simulating a much hotter, earlier Mars. The effects of changing temperature can be seen in Equation 3, where gravity is multiplied by temperature. Increasing the temperature has the same effect as increasing gravity, increasing the overall buoyancy.

2.3 RESULTS AND DISCUSSION

2.3.1 EARTH
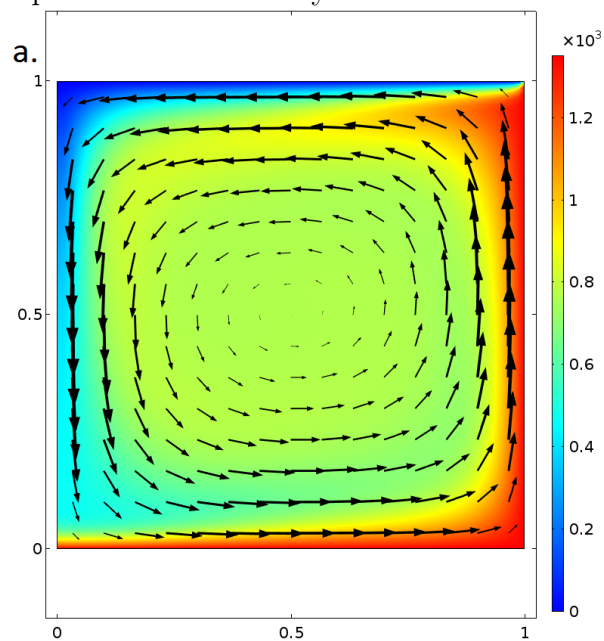
FIG. 30: The color bar on the right represents the calculated temperature (rainbow color) for the fluid in the Earth-like convection model, and ranges from 0 °C (blue) to 1350 °C (red). The physical size of the box is 400 km times the $x-$ and $y-$coordinates. The black arrows indicate the direction of the fluid and the magnitude (larger arrows indicates faster fluid motion).

Fig. 30 shows the temperature solution for the bottom- and right side-heated, top-cooled, Earth-like model for Rayleigh number equal to 10^5. The combination of heat sources from the bottom and right side of the square increased the temperature of the fluid near at $y = 0$ and along the boundary at $x = 1$, causing it to be buoyant Fig. 31. The buoyant fluid then

Illustration of Fluid Behavior

Heat sink, $T = 0$ °C

Heat source, $T = 1350$ °C

Heat source, $T = 1350$ °C

FIG. 31: A schematic diagram illustrating the overall fluid behavior based on the Earth temperature plot.

upwelled vertically to about $y = 0.95$, where it became cooler (from 1350 to 1000 °C), and more dense after encountering the cold top layer of the square. As a result of the increased density, the fluid started to become gravitationally unstable, and finally began to sink n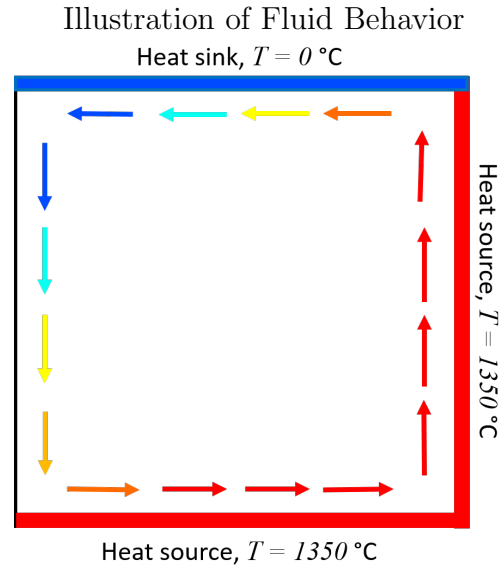ear $(x = 0, y = 0.85)$ at the temperature of 1000 °C. As it sank, the fluid then became warmer again while it traveled along the bottom $x = 1$ boundary.

Overall, the sum of all the fluid circuit paths formed a single convection cell moving counterclockwise in the square domain as also shown in Fig. 31, with the fastest velocities towards the outermost left and right edges of the square. The lowest temperatures were near the top and left boundaries, and the highest temperatures were near the bottom and right sides. The temperature at the center was calculated to be 1053 °C. The hot material rising along $x = 1$ may be thought of as analogous to a plume-like structure, the thermal boundary layer that increases in thickness from $(x = 1, y = 1)$ to $(x = 0, y = 1)$ is similar to the lithosphere, and the motion of the cool material sinking along $x = 0$ is comparable to that in a subduction zone.

2.3.2 MARS

Since the boundary conditions for Earth and Mars were identical, with the exception of the Prandtl number and thermal gradient, the overall convective flow pattern was also the

FIG. 32: (a-l) A series of Mars-like models, where the temperature T_h at the bottom and right side of the square increased in increments of 0.05, starting from $0.35T_\oplus$ (472.5 °C) and ending at $0.9T_\oplus$ (1215 °C). The color bar on the right hand side of the end figures represents the temperature of the fluid and ranges from 0 to 1350 °C. The thermal gradient for Mars is approximately half that of Earth. At $T_h = 675$ °C or at half the temperature of Earth, weak convection occurs on a Mars-like planet.

same, only weaker. At the lowest boundary temperature of $T_h = 472.5$ °C (Figure 32a), the domain was mostly isothermal at about 0 °C with a 135 °C layer developing between $(0 \leq x \leq 1, 0.9 \leq y \leq 1)$. For $T_h = 540$ °C (Fig. 32b) to $T_h = 607.5$ °C, (Fig. 32c) the temperature of that region increased to about 337 °C and it extended horizontally farther left. For $T_h = 675$ °C (Fig. 32d), around $(x = 0.25, y = 0.75)$, the fluid descended as its temperature dropped from 580 °C to 310 °C, and the fluid began to noticeably "curl in" on itself at point $(x = 0.5, y = 0.25)$. At $T_h = 742.5$ °C (Fig. 32e) and $T_h = 810$ °C (Fig. 32f), a similar flow pattern was repeated but the temperature increased on the bottom and right sides of the domain to about 675 °C, with the warmest fluid at $(x = 1, y = 0)$ and $(x = 1, y = 0.9)$. A weak convection cell was visible. The center of the domain at $T_h = 742.5$ °C was 337 °C and 405 °C for $T_h = 810$ °C.

As T_h is increased further, the temperatures throughout the model domain also increase, as expected. For example, at $T_h = 877.5$ °C (Fig. 32g) and $T_h = 945$ °C (Fig. 32h), the center of the convection cell was 526.5 °C and 540 °C. At $T_h = 1080$ °C, 1147.5 °C, and 1215 °C, the bottom and right side temperatures increased from 945 °C (Fig. 32j) to 1080 °C (Fig. 32k) to 1215 °C (Fig. 32l). The center of the domain at $T_h = 1080$ °C was 540 °C, and it increased to 567 °C at $T_h = 1147.5$ °C, and finally to 756 °C at $T_h = 1215$ °C. Convection became more vigorous from Fig. 32j to Fig. 32l.

Although there is no plate motion on Mars today, this study provides framework for investigating gravitationally driven mantle convection in the past. With increasing thermal gradients, structures similar to a plume, a lithospheric layer, and a subducting slab become more prominent.

2.4 FUTURE WORK

For this investigation, it was necessary to explore and fully understand a 2-D convection model, following studies like Schubert & Anderson (1985). A 3-D simulation of the entire mantle of Mars would provide a more realistic model. However, 3-D mantle convection simulations could take weeks to run. Large 3-D simulations may not even run on a desktop computer due to memory and architecture limitations and the computational complexity involved, and they thus could require a computer cluster or supercomputer. Additionally, larger crustal thickness requires cylindrical model geometries to accurately model a 2-D cross section of the mantle since a planet is spherical (Herein & Galsa, 2011).

Many factors affect convection, and thus future models should incorporate as many factors as possible. For example, the viscosity changes with depth in mantle, and the presence of

partial melting and compositional changes (especially the presence of water) both change the viscosity. In addition, planets have internal heat sources – the decay of radioactive elements further heats the mantle. Additional heat increases the convection speed.

Time dependence would also be interesting to examine in future work. A stationary model would perhaps miss some of the fluid behaviors that occur after more time has passed, such as the creation of a plume.

2.5 CONCLUSIONS

The 2-D models of incompressible Boussinesq fluid investigated in this thesis suggest that stable convection could occur in the interior of a Mars-like planet assuming the presence of sufficiently high ($T_h = 0.8T_\oplus$ or more) thermal gradients. This convection resembled structures similar to a plume (near heated boundaries), a lithospheric layer (near the cooled boundary), and a subducting slab (near the cooled boundary and the impermeable domain wall). Significant mixing of different temperatures was seen at approximately $T_h = 675$ °C. Increasing the temperature of the hot boundaries resulted in more rigorous convective motions and a hotter average temperature in the middle of the domain. These results are consistent with studies which find that, although the upper mantle of a planet like Mars (i.e., with Martian Prandtl number and Martian thermal gradient) has no current plate tectonics (i.e., surface plates moving laterally), it is possible that it had plate tectonics in the past.

GRAND TOUR OF THE SOLAR SYSTEM

Tour Download Locations

Body	Link	Creators
Solar System	http://www.digitalplanet.org/APP/SolarSystem_1m.kmz	Declan De Paor. Concept: Jeff Bennett
Mercury	http://messenger-education.org/googletours.php	NASA MESSENGER Mission Website
Venus	http://www.digitalplanet.org/APP/VenusInteriorLocal.kml	Mladen Dordevic, Vicki Hansen, Declan De Paor.
Earth	http://earth.google.com	Google Inc
Moon	http://earth.google.com	Google Inc
Mars	http://earth.google.com	Google Inc
Jupiter	http://bbs.keyhole.com/ubb/download.php?Number=372403 http://services.google.com/earth/kmz/jupiter_cassini_n.kmz	Frank Tayor, http://www.gearthblog.com
Io	http://www.geode.net/Io.kmz	Mladen Dordevic
Saturn	http://bbs.keyhole.com/ubb/download.php?Number=534324	James Stafford, http://www.barnabu.co.uk
Titan	http://www.digitalplanet.org/APP/Titan.kmz	Declan De Paor.
Uranus	http://www.gearthhacks.com/forums/downloads.php?do=file&act=down&id=31517	http://www.gearthhacks.com
Neptune	http://www.gearthhacks.com/forums/downloads.php?do=file&act=down&id=31516	http://www.gearthhacks.com
Pluto	http://geode.net/Pluto_New_Horizons.kmz	Declan De Paor. Imagery
Moons	http://www.barnabu.co.uk/the-many-moons-of-google-earth/	James Stafford, http://www.barnabu.co.uk/

In addition to the four terrestrial tours discussed in this paper, this table contains links to virtual globes for all planets and moons of the Solar System. The first row links to a 1:1 million scale model of the Solar System on Google Earth.

RAYLEIGH AND PRANDTL NUMBERS

Assuming that $\mu = \mu_0$, the Rayleigh number equals

$$\text{Ra} = \frac{(3440 \text{ kg m}^{-3})(2 \times 10^{-5} \text{ K}^{-1})(3.7 \text{ m s}^{-1})(400^3 \text{ km}^3)(1623.15 \text{ K})}{(10^{-6} \text{ m}^2 \text{ s}^{-1})(10^{19} \text{ Pa s})} \tag{9}$$

$$= 4.067 \times 10^6 \tag{10}$$

The Prandtl number equals:

$$\text{Pr} = \frac{\mu C_P}{k} \tag{11}$$

$$= \frac{(10^{19} \text{ Pa s})(1142 \text{ J kg}^{-1} \text{ K}^{-1})}{(4 \text{ W m}^{-1} \text{ K}^{-1})} \tag{12}$$

$$= 2.855 \times 10^{21} \tag{13}$$

REFERENCES

Anderson DL, Miller WF, Latham GV, Nakamura Y, Toksoz MN, Dainty AM, Duennebier FK, Lazarewicz, A. R., Kovach, R. L. Knight, T. C. D., 1977. Seismology on Mars. Journal of Geophysical Research 82, 4524–4546.

Barab, S.A., Hay, K.E., Barnett, M., and Keating, T., 2000. Virtual solar system project: Building understanding through model building. Journal of Research in Science Teaching 37, 719–756.

Bakas, C., Mikropoulos, T., 2003. Design of virtual environments for the comprehension of planetary phenomena based on students' ideas. International Journal of Science Education 25, 949–967.

Breuer, D., Spohn, T., 2006. Viscosity of the Martian mantle and its initial temperature: Constraints from crust formation history and the evolution of the magnetic field. Planetary and Space Science 54, 153–169.

Conrad, C.P., Lithgow-Bertelloni, C., 2002. How mantle slabs drive plate tectonics. Science 298, 207–209.

Corbin, J., Strauss, A., 2008. Basics of qualitative research (3rd ed.). Los Angeles, CA: Sage.

de Vahl Davis, G.V., Jones, I. P., 1983. Natural convection in a square cavity: a comparison exercise. International Journal of Numerical Methods in Fluids 3, 227–248.

De Jong, K. A., Scholtan, R., 1973. Gravity and tectonics. New York: Wiley & Sons

De Paor, D. G., Daniels, J., Tyagi, I., 2007. Five Geo-browser Lesson Plans. American Geophysical Union Fall Meeting, IN43A-0904

De Paor, D. G., 2008. Using Google SketchUp with Google Earth for Scientific Applications, Google Tech Talk, Retrieved from: https://www.youtube.com/v/6cVJqvsfxvo

De Paor, D. G., Whitmeyer, S. J., 2011. Geological and geophysical modeling on virtual globes using KML, COLLADA, and Javascript. Computers and Geosciences 37, 100–110.

De Paor, D. G., Wild, S. C., Dordevic, M. M., 2012. Emergent and animated COLLADA Models of the Tonga Trench and Samoa Archipelago: Implications for Geoscience Modeling, Education, and Research. Geosphere, 8, 491–506.

De Paor, D. G., Hansen, V. L., Dordevic, M. M., 2012. Google Venus. Geological Society of America Special Paper 492, 367.

De Paor, D. G., Coba, F., Burgin, S., 2016. A Google Earth grand tour of the terrestrial planets. Accepted for publication in the Journal of Geoscience Education, subject to revision.

De Paor, D. G., Dordevic, M. M., Karabinos, P., Burgin, S., Coba, F., Whitmeyer, S. J., 2016. Exploring The Reasons For The Seasons Using Google Earth, 3D Models, And Paper Plots. Accepted for publication in the International Journal of the Digital Earth, subject to revision.

Dordevic, M., Georgen, J., 2016. Dynamics of plume triple-junction interaction: Results from a series of three-dimensional numerical models and implications for the formation of oceanic plateaus. Journal of Geophysical Research: Solid Earth 121, 1316–1342.

Everitt, B.S., 2014. Repeated Measures Analysis of Variance. Wiley StatsRef: Statistics Reference Online. John Wiley & Sons, Ltd. doi: 10.1002/9781118445112.stat06585.

Fridleifsson, I. B., Bertani, R., Huenges, E., Lund, J. W., Ragnarsson, A., Rybach, L., 2008. The possible role and contribution of geothermal energy to the mitigation of climate change, O. Hohmeyer and T. Trittin, ed. Luebeck, Germany, 59.

Genova, A., Goossens, S., Lemoine, F. G., Mazarico, E., Neumann, G. A., Smith, D. A., Zuber, M. T., 2016. Seasonal and static gravity field of Mars from MGS, Mars Odyssey and MRO radio science. Icarus 272, 228–245.

Georgen, J.E., 2008. Mantle flow and melting beneath oceanic ridge ridge-ridge triple-junctions. Earth and Planetary Science Letters 270, 231–240.

Goettel, K. A., 1981. Density of the mantle of Mars. Geophysical Research Letters 8, 497–500.

Gomes, R., Levison, H. F., Tsiganis, K., Morbidelli, A., 2005. Origin of the cataclysmic Late Heavy Bombardment period of the terrestrial planets. Nature 435, 466–469.

Haskell, N. A., 1935. The Motion of a Viscous Fluid Under a Surface Load. Physics 6, 265–269.

Head, J. W., Kreslavsky, M. A., Pratt, S., 2002. Northern lowlands of Mars: evidence for widespread volcanic flooding and tectonic deformation in the Hesperian Period. Journal of Geophysical Research (Planets) 107, 3-1–3-29.

Herein, M., Galsa, A., 2011. The effect of different geometries on the thermal mantle convection. COMSOL Conference, Stuttgart, Germany, October 26-28, 2011.

Herrington, J., Kervin, L., 2007. Authentic learning supported by technology: Ten suggestions and cases of integration in classrooms. Educational Media International 44, 219–236.

Hesse-Biber, S., Dupuis, P., 2000. Testing hypotheses on qualitative data. The use of hyper research computer-assisted software. Social Science Computer Review 18, 320–328.

Holmes, A., 1931, Radioactivity and earth movements, Geological Society Glasgow Trans. 18, 559–606.

Ke, Y., Solomatov, V. S., 2006. Early transient superplumes and the origin of the Martian crustal dichotomy. Journal of Geophysics Research 110, E10001.

Kiefer, W. S., Li, Q., 2009. Mantle convection controls the observed lateral variations in the lithospheric thickness on present-day Mars. Geophysical Research Letters 36, L18203.

Koschmieder, E. L., 1993. Bénard Cells and Taylor Vortices. UK: Cambridge University Press. ISBN 0521-40204-2.

Küçöközer, H., 2008. The effects of 3D computer modelling on conceptual change about seasons and phases of the Moon. Physics Education 43, 632–636.

Leone, G., Tackley, P. J., Gerya, T. V., May, D. A., Zhu, G., 2014. Three-dimensional simulations of the southern polar giant impact hypothesis for the origin of the Martian dichotomy. Geophysical Research Letters 41, 8736–8743.

Li, Q., Kiefer, W. S., 2007. Mantle convection and magma production on present-day Mars: Effects of temperature-dependent rheology. Geophysical Research Letters 34, L16203.

Lingenfelter, R. E., Schubert, G. 1973. Evidence for convection in planetary interiors from first-order topogrpahy. Moon 7, 172–180.

Mardia, K. V., Kent, J. T., Bibby, J. M., 1979. Multivariate Analysis. San Diego, CA: Academic Press. ISBN 0-12-471250-9.

McGill, G. E., 2000. Crustal history of north central Arabia Terra, Mars. Journal of Geophysical Research 105, 6945–6959.

Messenger: MErcury Surface, Space ENvironment, GEochemistry, and Ranging. 1999-2015. Available at: `http://messenger.jhuapl.edu/the_mission/google.html` (accessed 13 August, 2015).

Mintz, R., Litvak, S. and Yair, Y. 2001. 3D-Virtual Reality in Science Education: An Implication for Astronomy Teaching. Journal of Computers in Mathematics and Science Teaching 20, 293–305

NASA. 2015. "NASA Suspends 2016 Launch of InSight Mission to Mars." `http://www.nasa.gov/press-release/nasa-suspends-2016-launch-of-insight-mission-to-mars`.

O'Neill, C., Lenardic, A., Weller, M., Moresi, L., Quinette, S., Zhang, S., 2016. A window for plate tectonics in terrestrial planet evolution? Physics of the Earth and Planetary Interiors 255, 80–92.

Reese, C.C., Solomatov, V. S., 2006. Fluid dynamics of local martian magma oceans. Icarus 184, 102–120.

Reid, I., Jackson, H. R., 2001, Oceanic spreading rate and crustal thickness. Marine Geophysical Researches 5, 165–172.

Ressler, S.J., 2004. Whither the Chalkboard? Case for a Low-Tech Tool in a High-Tech World. Journal of Professional Issues in Engineering Education and Practice 130, 71–73.

Rivoldini, A., Van Hoolst, T., Verhoeven, O., Mocquet, A., Dehant, V., 2011. Geodesy constraints on the interior structure and composition of Mars. Icarus 213, 451–472.

Robin, C., Jellinek, M., Thayalan, V., Lenardic, A., 2007. Transient mantle convection on Venus: The paradoxical coexistence of highlands and coronae in the BAT region. Earth and Planetary Science Letters 256, 100–119.

Ruiz, J., Tejero, R., McGovern, P. J., 2006. Evidence for a differentiated crust in Solis Planum, Mars, from lithospheric strength and heat flow. Icarus 180, 308–313.

Schubert, G., Anderson, C. A., 1985. Finite element calculations of very high Rayleigh number thermal convection. Geophysical Journal of the Royal Astronomical Society 80, 575–601.

Schubert, G., Turcotte, D. L., Olson, P., 2001. Mantle Convection in the Earth and Planets, 1st ed. Cambridge University Press.

Sekhar, P., King, S. D., 2014. 3D spherical models of Martian mantle convection constrained by melting history. Earth and Planetary Science Letters 388, 27–37.

Sewasew, D., Mengestie, M., Abate, G., 2015. A comparative study on power point presentation and traditional lecture method in material understandability, effectiveness and attitude. Educational Research and Reviews 10, 234–243.

Sleep, N. H., 1994. Martian plate tectonics. Journal of Geophysics Research 99, 5639–5655.

Solomon, S. C., Head J. W., 1989, Estimating lithospheric thermal gradient on Mars from elastic lithosphere thickness: New constraints on heat flow and mantle dynamics. Lunar and Planetary Science Conference 20, 1030.

SPSS, C. 1990. Statistical Package for Social Science.

Stewart, A. J., Schmidt, M. W., van Westrenen, W., Liebske, C., 2007. Mars: A new core-crystallization regime. Science 316, 1323–1325.

Turcotte, D. L., Schubert, G., 2002. Geodynamics, 2nd ed. UK: Cambridge University Press, ISBN:978-0521661867.

Wang, X., 2004, Infinite Prandtl number limit of Rayleigh-Bénard convection. Communications on Pure and Applied Mathematics 57, 1265–1282.

Watters, T. R., McGovern, P. J., Irwin III, R. P., 2007, Hemispheres Apart: The Crustal Dichotomy on Mars. Anual Review of Earth and Planetary Sciences 35, 621–652.

Wegener, A., 1922, Die Entstehung der Kontinente und Ozean. Available: `https://lccn.loc.gov/unk83068007`.

Whitmeyer, S.J., Bailey, J., De Paor, D.G., Ornduff, T., (eds.) 2012. Google Earth and Virtual Visualization in Geoscience Education and Research. Geological Society of America Special Paper 492, 468.

Zhong, S., Zuber, M. T., 2001. Degree-1 mantle convection and the crustal dichotomy on Mars. Earth and Planetary Science Letters 189, 75–84.

Zhong, S., 2009. Migration of Tharsis volcanism on Mars caused by differential rotation of the lithosphere. Nature Geoscience 2, 19–23.

Zuber, M. T., 2001. The crust and mantle of Mars. Nature 412, 220–227.

VITA

Filis Coba

Department of Physics

Old Dominion University

Norfolk, VA 23529

From a young age, I was curious about the mechanics of the universe, initially understanding through drawing and painting then progressing more towards the analytical methods of physics, geophysics, and astronomy.

EDUCATION

Old Dominion University (anticipated Aug., 2016)

M.S. in Physics

Advisor: Declan De Paor in collaboration with Jennifer E. Georgen Thesis: Simulation of Mars-Like Mantle Convection & Implication for Gravity-Driven Tectonics

Central Connecticut State University (2010)

B.S. in Physics, Minors in Mathematics and Art

PUBLICATIONS

De Paor, D. G., **Coba, F.** & Burgin, S. 2016, *"A Google Earth grand tour of the terrestrial planets"*. Accepted for publication in the Journal of Geoscience Education, subject to revision.

De Paor, D. G., Dordevic, M. M., Karabinos, P., Burgin, S., **Coba, F.**, Whitmeyer, S. J. 2016, *"Exploring The Reasons For The Seasons Using Google Earth, 3D Models, And Paper Plots"*. Accepted for publication in the International Journal of the Digital Earth, subject to revision.

Typeset using LaTeX.